DEVELOPMENT AND EVALUATION OF SILICONE MEMBRANE AS AERATORS FOR MEMBRANE BIOREACTORS

Xolani Proffessor Mbulawa

B Tech (Eng)

Submittend in fulfilment of the
requirements for the degree of
Master of Technology
in the
Department of Chemical Engineering
Durban University of Technology, Durban

SUPERVISOR

Prof VL Pillay (PhD)

CO SUPERVISOR

EP Jacobs (PhD)

June 2005

Declaration

I hereby declare that this dissertation is my own work, unless stated to the contrary I the text, and that it has not been submitted for a degree to any other University or Institution.

Xolani Proffesssor Mbulawa

This dissertation is

dedicated to my

Mother

Acknowledgements

I wish to express my sincere gratitude to the following people, for their contributions towards this dissertation.

i. Dr VL Pillay, my supervisor and Prof EP Jacobs my co-supervisor for their invaluable input in terms of guidance, assistance, discussions and encouragement.

ii. Members of the Water Technology Group and the staff of the Department of Chemical Engineering for their general assistance. Special mention to Sadhana Vallabh for proof reading this dissertation.

iii. Eddie Davies and Patrick Chamane from Mechanical Engineering workshop at DIT for their assistance in constructing some of the experimental set-up.

iv. Sello Phalime for his assistance and encouragement.

v. NRF and DoL Scarce Skills for sponsoring me.

Abstract

In bubble-less aeration oxygen diffuses through the membrane in a molecular form and dissolves in the liquid. Oxygen is fed through the lumen side of silicone rubber tube. On the outer surface of the membrane there is a boundary layer that is created by oxygen. This then gets transported to the bulk liquid by convective transport created by water circulation through the pump. The driving force of the convective transport is due to concentration difference between the dissolved oxygen in water and oxygen saturation concentration in water at a particular temperature and pressure.

The design of a membrane aerated bioreactor needs an understanding of the factors that govern oxygen mass transfer. It is necessary to know the effects of operating conditions and design configurations. Although various methods of bubble-less aeration have been reported, there still exists a lack of knowledge on the immersed membrane systems.

This study is aiming at contributing to the development of an immersed membrane bioreactor using silicone rubber tubular membrane as means of providing oxygen. The secondary objective was to investigate the influence that the operating conditions and module configuration have on the system behaviour.

From the experimental study, the characteristic dissolved oxygen -time curve show that there is a saturation limit equivalent to the equilibrium dissolved oxygen concentration, after which there is no increase in dissolved oxygen with time. At ambient conditions the equilibrium dissolved oxygen is approximately 8 mg/L. This is when water is in contact with air at one atmospheric pressure. At the same conditions the equilibrium dissolved oxygen concentration when water is in contact with pure oxygen is approximately 40

mg/L. This is why all the experiments were conducted from 2mg/L dissolved oxygen concentration in water, to enable enough time to reach equilibrium so as to determine mass transfer coefficient. The most important parameters that were investigated to characterise the reactor were, oxygen supply pressure, crossflow velocity, temperature and module orientation.

Observations from the experimental study indicated that when the system is controlled by pressure, crossflow does not have a significant effect on mass transfer. When the system is controlled by the convective transport from the membrane surface to the bulk liquid, pressure does not have a significant effect on mass transfer. All four effects that were investigated in the study are discussed.

Table of contents

Chapter 5: Results and discussion

List of Figures

List of Tables

Nomenclature

A	Surface area of fibres available for mass transfer
DO	Dissolved oxygen concentration
C	Dissolved oxygen concentration in water
C*	Equilibrium oxygen concentration in water
Co	Initial DO concentration
Ct	DO concentration at any time t
Q	Water flowrate
T	Temperature
t	Time
δ	Concentration boundary layer thickness
Re	Reynolds number
Sh	Sherwood number
Sc	Schmidt number
d	Diameter of hollow fiber
D	Diffusion coefficient
H	Henry's law constant
J	Flux
K	Overall mass transfer coefficient
K_L	Liquid phase mass transfer coefficient

K_m	Membrane phase mass transfer coefficient
K_g	Gas phase mass transfer coefficient
K_p	Permeability
P_g	Pressure of gas
V_w	Volume of the reactor
υ	Kinematics viscosity of water

Chapter 1

INTRODUCTION

1.1 BACKGROUND

Aerobic biological processes are the key to wastewater treatment and are deployed in the activated sludge process, which is the most common treatment technique worldwide. This involves the treatment of organisms in the presence of oxygen. The aerobic environment in the conventional activated sludge process is achieved by the use of diffused or mechanical aeration. These processes bubble air through the system to provide oxygen.

Due to the low solubility of oxygen in water, the treatment of high oxygen demanding wastewaters by aerobic processes is often limited by insufficient oxygen when using atmospheric air. By switching from air to high purity oxygen, the rate of oxygen mass transfer can be significantly increased. A number of advantages, such as increased bacterial activity, decreased sludge volume, reduced aeration tank volume and improved sludge settleability, have been reported for this process (Metcalf and Eddy, 1991). However, conventional oxygenation devices have high power requirements associated with the need for high rates of mixing. There are other disadvantages to this process such as stripping of volatile organic compounds, foaming of industrial wastewaters and poor oxygen utilization efficiency due to oxygen bypassing the bed in the form of bubbles.

Limitations presented by the above on conventional aeration devices led to the development of a process that is more effective in oxygen transfer. Schaffer *et al.*, (1960) investigated the use of plastic film as a mode of aeration and noted that slime growth developed on the plastic. More recently, the use of hollow fibres for oxygen transfer has

been reported (Ahmeed and Semmens, 1996). The advantages of membranes over conventional dispersion-phase contactors, such as packed towers, spray towers or bubble columns, are the smaller shear stresses in the liquid phase, much larger interfacial areas per unit volume, the independent control of phase flow rates without flooding or loading problems, and the constant interfacial area for transfer over the entire operating range of flow rates.

Two types of gas permeable membranes are used for membrane-based gas absorption processes: nonporous silicone rubber membranes and microporous membranes. Micro porous membranes have the advantage of providing very high gas permeabilities. In addition to that, membranes can be manufactured as small-diameter (100-400 :m) hollow fibres that can provide a very high interfacial area per unit volume. Silicone rubber membranes can be operated at high transmembrane pressure without bubble formation. However in order to withstand higher pressure differences, microporous hollow fibres can be coated by an ultra thin layer of silicone rubber (A Van der Walt, 1999).

1.2 PROJECT OBJECTIVES

The overall objective of the project was to evaluate the use of silicone rubber membranes as aerators in membrane bioreactors (MBR's).

The specific objectives of the study were to determine the

i) Effect of oxygen supply pressure on mass transfer
ii) Effect of membrane geometry within the reactor.
iii) Effect of crossflow velocity on mass transfer.
iv) Effect of temperature on mass transfer.

1.3 APROACH

An immersed membrane reactor was set up with silicone rubber tubes with a transfer area of 0.228m^2 in a rectangular frame that enabled the membrane to be positioned in an axial direction of liquid flow and also in a transverse direction to flow. The equipment used was a 30 L rectangular Perspex tank, a DO meter (Hanna HI 9143), and a rectangular stainless steel membrane manifold. Mixing was achieved by using a centrifugal pump with a capacity of 2m^3/h

Oxygen was supplied to the membranes from an oxygen cylinder controlled by a regulator. Dissolved oxygen was measured in the tank using a DO probe. Sodium sulphite was used to deplete oxygen in water and cobalt was used as a catalyst. Change in dissolved oxygen was monitored in the tank to determine the effect of the above-mentioned effects.

1.4 THESIS OUTLINE

The remainder of this dissertation is divided into five chapters.

Chapter two gives background information on membrane bioreactors and the types of membranes used and limitations presented by those membranes. It also introduces methods that were used to overcome those limitations and finally the need to have this investigation.

Chapter three gives an experimental methodology used to achieve the required objectives with some of the difficulties encountered in developing the final experimental apparatus.

Chapter four gives theoretical derivation of mass transfer models used in the study.

Chapter five discusses the results

Chapter six summarizes the findings and presents some recommendations.

Chapter 2

LITERATURE REVIEW

2.1 Membrane bioreactors (MBR)

Membrane bioreactors are the combination of a suspended growth reactor and membrane filtration device into one single process. The membrane unit can be immersed in the bioreactor (Figure 2.1) or external to, as side stream operation (Figure 2.2). The coupling of a membrane to a bioreactor has attracted increased interest both academically and commercially because of the inherent advantages the process offers over conventional biological wastewater treatment systems.

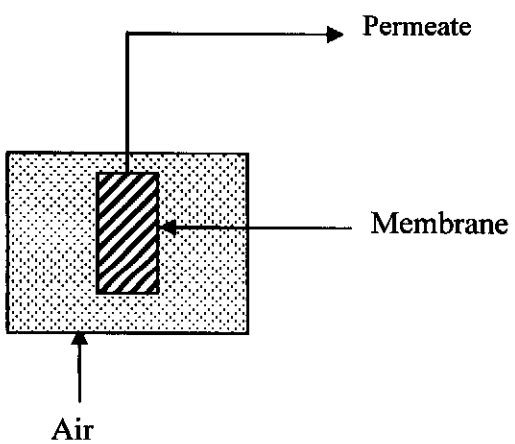

Figure 2.1: Schematic of an immersed membrane bioreactor

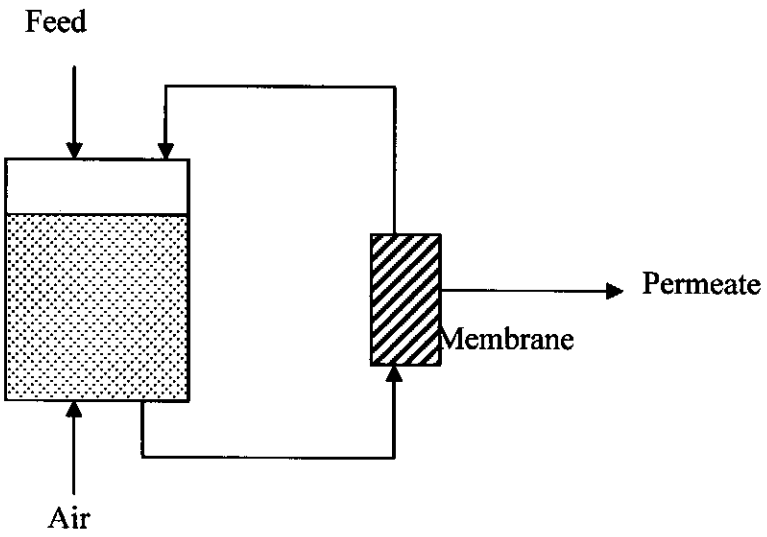

Figure 2.2: Schematic of a side stream membrane bioreactor

Major advantages of MBR are process intensification and product water quality, also the permeate from the membrane is free from solids and macro-colloidal material. However the advantages described above are offset by several disadvantages which have to date restricted the widespread application of MBR technology. The most significant disadvantage being the cost of the membrane. Operational problems also exist. Common to all membrane systems is fouling, moreover the high biomass concentrations that are a facet of the process can result in aeration problems. The majority of the air supplied is required for cell maintenance, rather than for aerobic degradation.

2.2. Membrane aerated bioreactors

Research into membrane aeration bioreactors (MABR) has been driven by the need to enhance the performance capabilities and the scope of application of biological wastewater treatment processes. Wastewater treatment processes using high purity oxygen have a greater volumetric degradation capacity compared to conventional air aeration processes. The MABR uses a gas permeable membrane to supply high purity oxygen directly to a biofilm without bubble formation. In the MABR process the capability of the biofilm to retain high concentrations of active bacteria is coupled with the high transfer rate of oxygen to the biofilm. Therefore the MABR is an attractive alternative to conventional processes for the treatment of high oxygen demanding wastewaters.

2.2.1. Membrane Aeration in the MABR process

Dense gas permeable, hydrophobic and composite membranes are used to transfer oxygen to degradative bacteria present in the bioreactor without bubble formation (Figure 2.3).The membrane usually also acts as support media for biofilm development at the membrane/ liquid interface. Wastewater flows over the outer surface of the biofilm and counter-diffusion of oxygen and pollutant occurs. Oxygen is utilized during the biodegradation of pollutants within the biofilm. High purity oxygen is usually used in MABR processes.

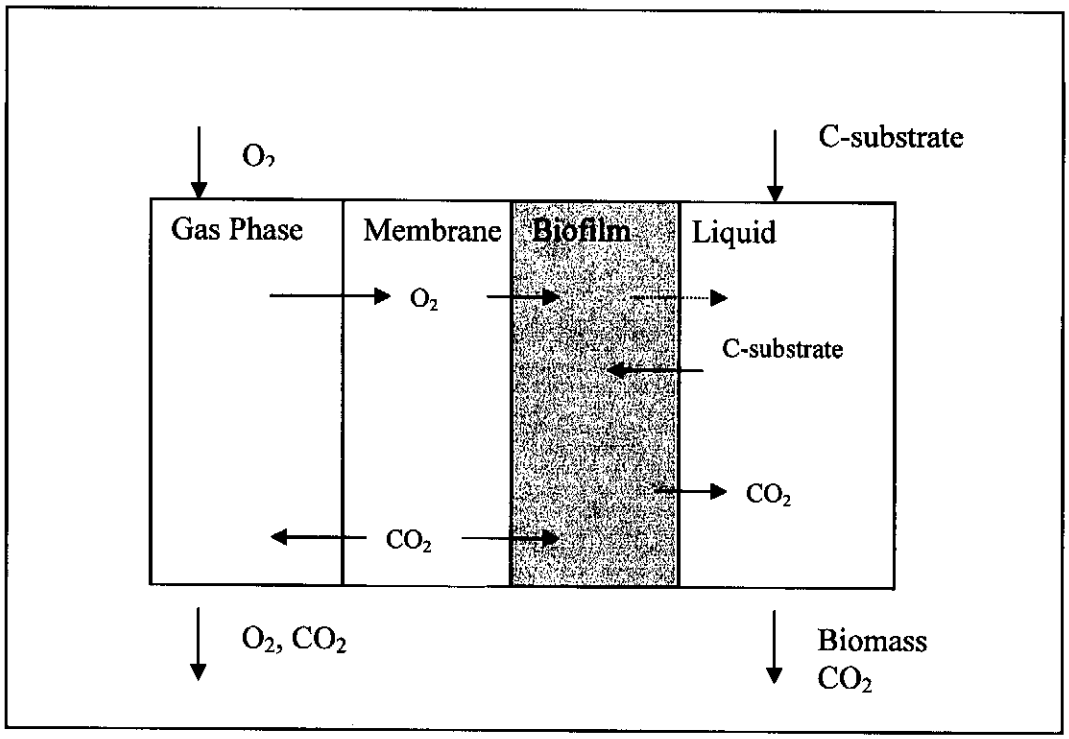

Figure 2.3: Schematic diagram of MABR.

Plate and frame, tubular and hollow fibre membrane configurations have been used in MABR processes. The specific surface area of such membranes ranges from $19m^2/m^3$ plate and frame to a hollow fibre unit of $5108m^2/m^3$, far greater than in conventional attached – growth bioreactors (Pankhania *et al.,* 1994). Research has focused on hollow fibres, with the gas on the lumen side and the wastewater on the shell side of the fibres. These provide a high surface area for oxygen transfer and biofilm formation while occupying a relatively small volume within the bioreactor. Pressurized hollow fibre and tubular membranes have been investigated in dead-end and flow - through modes of operation.

Though 100 % oxygen transfer efficiency can be achieved when using hydrophobic dead-end hollow fibres their use has been avoided until recently. This was due to condensate formation in the lumen, reducing the active membrane surface area for oxygen mass transfer (Cote *et al.*, 1989). Fluidised hollow fibre bundles, with individual fibres independent of one another, are known to be less susceptible to clogging (Ahmed *et al.*, 1992).

Oxygen diffusion through dense gas permeable membrane material can be achieved at high gas pressures without bubble formation. Work using dense polymers has largely focused on tubular silicone membranes. These membranes have high oxygen permeabilities, and are very resistant to chemical and mechanical abrasion (Debus *et al.*, 1992). It has previously been suggested that biofilm formation does not occur on silicone rubber (Cote *et al.*, 1989). However, several investigations demonstrated that silicone rubber is a suitable material for biofilm attachment during diffusion of oxygen through the membrane material (Debus *et al.*, 1992).

In the MABR process, the oxygen transfer rate can be enhanced by increasing either the mass transfer driving force (C*-C), the membrane surface area (A) or the overall mass transfer coefficient (K). For a given set of operating conditions, increasing the membrane surface area yields greater oxygen transfer rates without requiring more power and therefore also improves the standard aeration efficiency (SAE). Maintaining a high mass transfer driving force can be achieved by supplying oxygen at high partial pressure (P_T) or keeping the dissolved oxygen concentration at zero (C). In conventional aeration devices the oxygen feed pressure (P_T) is limited by atmospheric and hydrostatic conditions.

2.3 Membranes

2.3.1Membrane definition

A membrane can be described as a material through which one type of substance can pass more readily than others, thus presenting the basis of a separation process. For many processes membranes act to reject pollutants, which may be suspended or dissolved and allow purified water through it, or transfer gas to the wastewater, as in the bubble-less oxygenation (Brindle *et al.,* 1998)

2.3.2 Membrane structure and materials

The materials used to fabricate a membrane for any application have to produce the required separation, have a high degree of selectivity, be strong to handle the operating pressures and have a high permeate throughput. It does however make it very difficult to find a membrane that can exhibit all these required properties. In most cases membranes that have high throughput also have poor separation. The selectivity of membrane is dependent on the pore size distribution of a membrane, the wider the pore size distribution the poorer the selectivity.

The chemical composition and physical structure of a membrane has significant implication for the application of that membrane to a particular process. There are dense and porous membranes and each membrane type is intended for a particular application ranging from removal of ions in a solution to removal of particulates in suspension. The dense membranes depend on the physcio-chemical interactions to effect separation while the porous one depends on the sieving mechanism to effect separation.

2.3.3 Membrane types and process technologies

The diversity of membrane based separation systems makes it difficult to categorize them clearly. The systems are typically labelled either on the basis of type of membrane employed, or the driving force applied to assist penetrant transport through the membrane. The types of membranes used for separation are classified as porous or non-porous. With each type of membrane used, further classification is based on the type of applied driving force for the penetrant.

2.3.3.1 Porous Membranes

Porous membranes are studied in terms of their pore size. These are classified as either micro porous for micro filtration] or ultra porous for ultrafiltration. The principle of operation in porous membranes can be described as molecular sieving, where large molecules are excluded from the pores by virtue of their pore size.

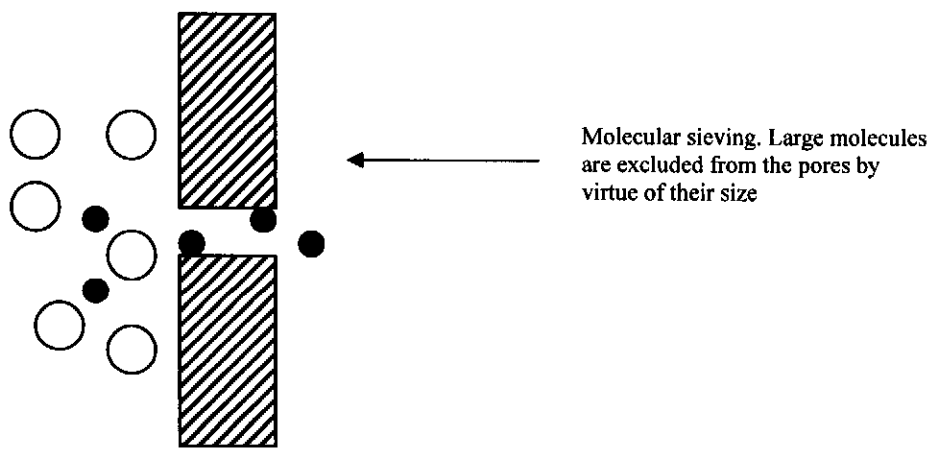

Figure 2.4 Operating principles for a porous membrane

2.3.3.2 Non-porous or Dense Membranes

Non-porous membranes primarily consist of polymer membranes. The non-porous structure of the polymer is related to the non-continuous passage present in the polymer chain matrix. These passages are created and destroyed due to thermally induced motion of the chains. Therefore, the transport of a penetrant is based on its movement through these passages. The effects of penetrant activity (driving force) and operating conditions then play an important role in governing the transport rate and separation property of the membrane.

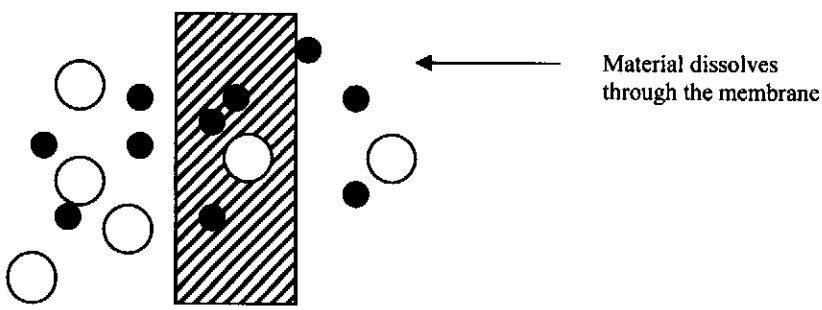

Figure 2.5 Operating principles for a non -porous membrane

The first non-porous membrane used for separation purposes was natural rubber. A number of approaches have been used over the years to describe the way in which low molecular weight species penetrate nonporous rubber membranes. The mechanism of the permeation process entails solution of the penetrant in the upstream surface of the membrane, diffusion through the membrane by "colloidal diffusion" followed by evaporation from the downstream membrane surface

As mentioned earlier, the classification of non-porous membrane separation processes is based on the applied driving force. The classification for non-porous membrane separation processes is summarized in Table 2.1. Some of the processes are also applicable to porous membranes.

Table 2.1: Membrane separation processes for non-porous membranes.

Process Name	Applied Driving Force
Pervaporation	Vapour pressure
Gas permeation	Pressure
Reverse Osmosis	Pressure
Electro dialysis	Electric potential

Membrane technologies like microfiltration and ultrafiltration use the sieving mechanism to remove particulates and dissolved matter from suspensions. Nanofiltration and reverse osmosis membrane are processes that use physcio-chemical interactions to separate ions from water. Microfiltration in particular is capable only of removing particulates and suspended matter because of its pore size (around 0.05:m). These porous membranes (MF and UF) are generally used in membrane bioreactors to separate the effluent from the biomass. The application of these membrane technologies (MF and UF) in the filtration of activated sludge is in the process of replacing the use of gravity clarifiers/settlers in the activated sludge process (Churchouse, 1997).

The micro filtration membranes can be made from either organic or inorganic materials. Inorganic membranes are produced by sintering and pressing of powders onto a pre-prepared porous support. The membranes are very expensive to produce using this method particularly if a narrow pore size distribution is required .The organic membranes are relatively simpler to produce compared to the inorganic membranes. Organic membranes can be modified to suit a particular application by altering the surface charges on the membranes.

2.4 Silicone rubber membranes

Previous research showed that skinless polysulphone membranes coated with a layer of silicone rubber improved mass transfer of oxygen through the membrane (Van der Walt, 2001). Tubular silicone membranes have higher oxygen permeabilities and are very resistant to chemical and mechanical abrasion due to their polymer structure. Cote *et al.*, (1989) suggested that biofilm formation does not occur on silicone rubber membrane due to either the hydrophobic nature of the silicone or biomass poisoning by high oxygen concentrations at the membrane wall. However, several investigations have demonstrated that silicone is a suitable material for biofilm attachment during diffusion of oxygen through the membrane material (Debus *et al.*, 1992). Also, tubular silicone rubber membranes can be operated at higher transmembrane pressure without bubble formation.

2.4.1 Mechanism of transport through silicone rubber

The mechanism for transport of components through dense membranes such as silicone is that of "solution diffusion". Oxygen transport through silicone rubber is based on oxygen dissolution in the membrane, followed by diffusion of the gas through the thickness of the membrane, under the applied driving force. High permeabilities are due to the fact that compounds such as oxygen are four to five times more soluble in silicone than in water. Silicone membranes are not available with wall thicknesses as thin as that of microporous membranes, but have the advantage of allowing high intra-membrane oxygen pressure to be used.

2.5 Theory of membrane permeability through silicone rubber

2.5.1 Fundamentals

The first study on gas permeation through polymer dates back to 1829, when Thomas Graham observed the inflation of a wet pig bladder with CO_2. It was in 1866, when Graham formulated the "Solution diffusion process", where he postulated that the permeation process involved the dissolution of penetrant, followed by transmission of the dissolved species through the membrane. The other important observations made at that time were:

1. Permeation was independent of pressure
2. Increase in temperature lead to decrease in penetrant solubility, but made the membrane more permeable.
3. Prolonged exposure to elevated temperature affected the retention capacity of the membrane.
4. Variation in membrane thickness altered the permeation rate but not the separation characteristics of the polymer.

Fick in 1855, by analogy to Fourier's law of heat conduction, proposed the law of mass diffusion where the penetrant flux (J), for one-dimensional diffusion, is represented as.

$$J = \frac{Q_g}{A} = -D\frac{\delta C}{\delta x} \tag{2.1}$$

where Q_g = volumetric flow rate of gas

A = surface area

D = diffusivity of gas

$\frac{\delta C}{\delta x}$ = concentration gradient applied across the membrane

and C = concentration of dissolved gas

Stefan and Exner showed that gas permeation through the membrane was proportional to the solubility coefficient (S) and Fick's diffusion coefficient (D)

$$K_p = SD \tag{2.2}$$

where K_p = permeability coefficient

Henry's law states that a gas dissolves in a dense membrane (e.g. silicone rubber) according to the following equation:

$$C = SP_g \tag{2.3}$$

where S is the solubility coefficient and P_g is the gas pressure.

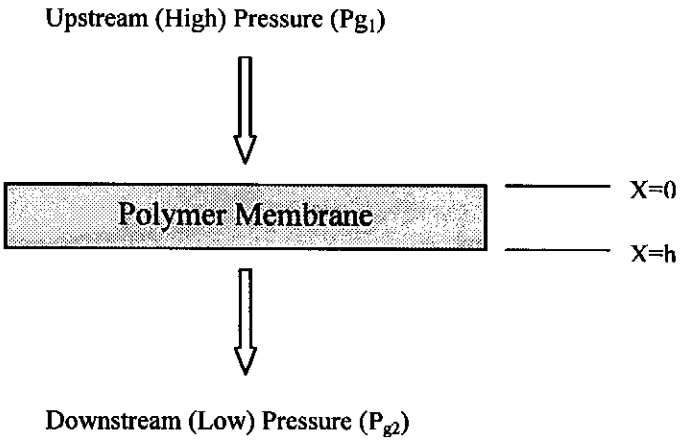

Figure 2.6: Schematic representation of gas transport through membrane.

Wroblewski further showed that under steady state conditions, and assuming diffusion coefficient to be independent of concentration, the gas permeation flux, illustrated in figure 2.7, could be expressed as

$$J = K_p \frac{(P_{g1} - P_{g2})}{X} = K_p \frac{\Delta P}{X} \qquad (2.4)$$

Where $\frac{\Delta P}{X}$ is the applied pressure gradient across the membrane thickness (X), K_p is defined as the gas permeability of the membrane. The conventional unit for expressing K_p is Barrers, where 1 Barrer $=10^{-10}$ (cm^3 (STP)/ cm.sec.cmHg).

2.6 Mass transfer coefficients

For oxygen to be transported from the fiber lumen to the targeted bulk liquid, it must diffuse through the membrane wall, and through the liquid boundary layer as shown in Figure 2.6

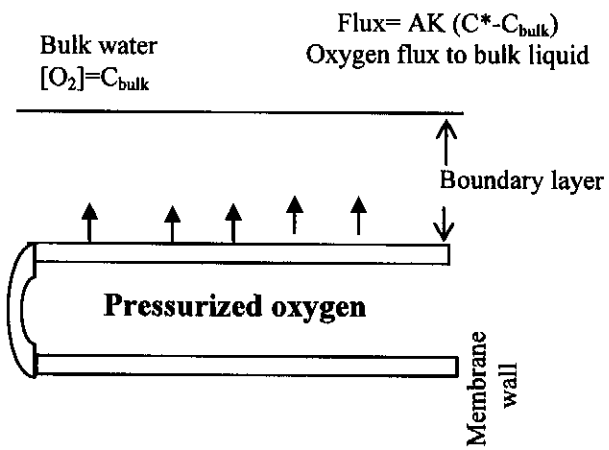

Figure 2.7 Schematic of diffusion process, oxygen diffusing from fiber wall.

The overall resistance to mass transfer is composed of three separate resistances in series: (1) the gas film resistance; (2) membrane resistance; and (3) liquid film resistance. The gas film resistance is negligible (Yang and Cussler, 1986) and the membrane resistance can be small if the membrane walls are completely porous. However, the membranes used in this study did provide a significant membrane resistance due to the composite structure of the polymer. The liquid film resistance is also important being dependent only on the concentration boundary-layer thickness and the diffusivity of oxygen in water (Hanratty, 1991).

$$k_L = \frac{D}{\delta} \qquad (2.5)$$

where k_L = liquid phase mass transfer coefficient

D = diffusivity of oxygen in water

δ = concentration boundary layer thickness

Thus, a larger diffusivity or a thinner boundary layer will increase both the liquid-side mass transfer coefficient and the overall rate of oxygen transfer.

A minimum boundary layer thickness will maximise oxygen transfer rates. For a given fiber, the boundary layer thickness can be manipulated by controlling the water velocity and orientation of the fibres relative to the oncoming water velocity. Hollow fiber membranes can be oriented such that the long axis of the fiber is parallel to the direction of the flowing water or at an angle to the direction of the water flow. These are classified as parallel (axial) flow and cross flow, respectively. The boundary layer on a parallel flow fiber develops over the entire length of the fiber and is therefore thicker than the boundary layer on a crossflow fiber, which has only half the fiber circumference to develop.

The existing correlations for liquid-film coefficients as determined from experiments on various types of physical modules are given in Table 2.2. It can be seen from the table that, in cross flow, the Reynolds power number dependence typically ranges from approximately 0.3 to 0.4. In parallel flow the Reynolds number dependence seems to be higher. The increase in Reynolds number dependence from cross to parallel flow is expected since boundary layer development (i.e., liquid film resistance) plays a more dominating factor in parallel flow.

Table 2.2. Comparison of Empirical Relationships

Flow	Reference	Correlation	Comment
Parallel	Yang and Cussler (1986)	$Sh = 1.25[Re(de/L)]^{0.93}Sc^{0.33}$	Water flow inside or outside of fibres. Driving force provided by a vacuum or nitrogen sweep gas
	Ahmed and Semmens (1992)	$Sh = 0.11Re^{0.81}Sc^{0.33}$ $Sh = f_v(7.46)Re^{0.26}$	Fibres sealed at one end and water flow outside fibres
	Johnson et al. (1997)	$Sh = 1.38\ Re^{0.40}Sc^{0.33}$	Composite membranes sealed at one end
Cross- flow	Yang and Cussler (1986)	$Sh = 1.38Re^{0.40}Sc^{0.33}$	Water flow inside or outside of fibres. Driving force provided by a vacuum or nitrogen sweep gas
	Ahmed and Semmens (1996)	$Sh = 1.45\ Re^{0.32}Sc^{0.33}$	Microporous membranes sealed at one end

Chapter 3

MATHEMATICAL MODELS DESCRIBING MASS TRANSPORT

3.1 Introduction

In this section the theoretical mass transfer correlations for the following experimental set-ups will be derived:

Shell and Tube

- Absorption of gas, with gas in dead end mode (tube side) and water in flow through mode (shell side);
- Absorption of gas, with gas in dead end mode (tube side) and water in recycle mode (shell side).

Immersed membrane reactor

- Absorption of gas, with gas in dead end mode.

Mass transfer in dense membranes takes place at the interface between the surface of the membrane and the liquid phase. The driving force for mass transfer across the interface is proportional to the concentration difference of the diffusing gas between the phases. At equilibrium, the concentration in the gas phase, C_g is related to Henry's law constant, H, by

$$C_g = HC^* \qquad (3.1)$$

3.1.1 Absorption of oxygen, with gas in dead-end mode and water in once-through mode

Water is pumped through the shell side of the membrane and oxygen on the tube side. Dissolved oxygen concentration (DO) is measured on the exit point of the module, to determine the change in DO concentration over the entire length of the module.

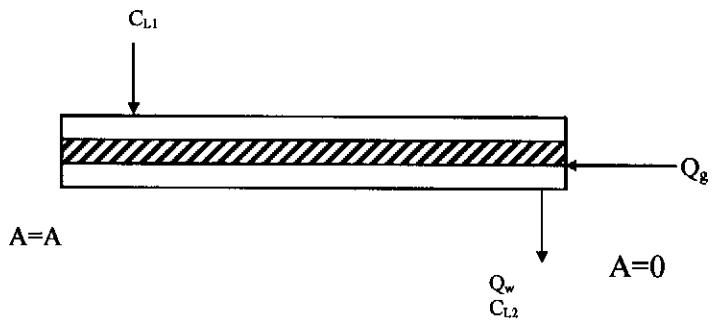

Figure 3.1: Schematic representation of liquid flowing through a membrane module with gas in dead-end mode.

Consider absorption of oxygen by water flowing outside of the module (shell). The material balance on the dissolved (DO) is given by:

Accumulation = Flow in – Flow out + Absorption of oxygen

At steady state, accumulation equals zero.

$$0= -Q_w(dC) + K(C^* - C)dA$$

where dC is the change in DO concentration, K is the overall mass transfer, C* is the concentration in the liquid phase in equilibrium with the gas and C is the arbitrary concentration of the liquid on the shell side. C changes throughout the length of the pipe, hence dA.

$$\frac{dC}{C-C^*} = -\frac{K}{Q_w}dA \tag{3.2}$$

Integrating equation (1) from C =C_1 to C=C_2 and A=0 to A=A

$$\int_{C_1}^{C_2} \frac{dC}{C-C^*} = -\frac{K}{Q_w}\int_0^A dA$$

$$\ln\frac{C_2-C^*}{C_1-C^*} = -\frac{K}{Q_w}A$$

Therefore:
$$K = -\frac{Q_w}{A}\ln\frac{C_2-C^*}{C_1-C^*} \tag{3.3}$$

3.1.2 Absorption of oxygen with gas in dead-end mode and water in recycle-mode.

Water is pumped from the stirred reservoir through a membrane module and returned to the reservoir. The dissolved oxygen concentration (DO) in the water reservoir is monitored over time so that the overall mass transfer coefficient can be calculated.

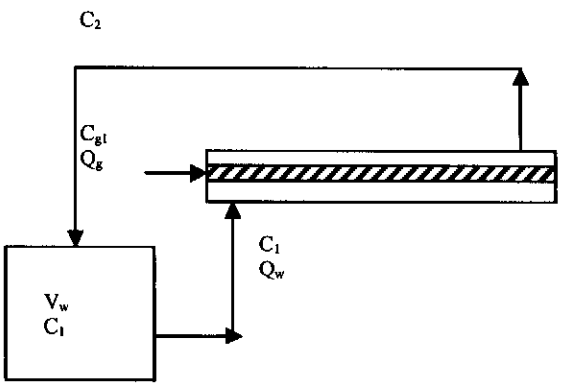

Figure 3.2: Schematic representation of oxygen absorption, with gas in dead-end mode and water in recycling mode.

A mass balance on dissolved oxygen around the tank describes the change in concentration with time.

Accumulation = Flow in – Flow out

$$V_w \frac{dC_1}{dt} = Qw(C_2 - C_1) \qquad (3.4)$$

where V_w is the tank volume (L), C_1 and C_2 are concentrations on the exit and entrance of the tank respectively (mg/L) and Qw is the water flowrate.

Rearangement of equation (3.3) yields:

$$C_2 = e^{(-KA/Q_w)}(C_1 - C^*) + C^*$$

Substitute for C_2 in equation (3.4):

$$V_w \frac{dC_1}{dt} = Q_w\left[(e^{(-KA/Q_w)}(C_1 - C^*)) + C^* - C_1\right]$$

$$\frac{dC_1}{dt} = \frac{Q_w}{V_w}\left[(e^{(-KA/Q_w)}(C_1 - C^*)) - (C_1 - C^*)\right]$$

$$\frac{dC_1}{dt} = \frac{Q_w}{V_w}(C_1 - C^*)\left[e^{(-KA/Q_w)} - 1\right]$$

$$\frac{dC_1}{C_1 - C^*} = \frac{Q_w}{V_w}\left[e^{(-KA/Q_w)} - 1\right]dt$$

Integrating the above expression from $C_1 = C_{1(t(0))}$ to $C_1 = C_{1(t(t))}$ and t=0 to t=t yields:

$$\int_{C_{1(0)}}^{C_{1(t)}} \frac{dC}{C_1 - C^*} = M \int_0^t dt$$

$$\ln \frac{C_{1(0)} - C^*}{C_{1(t)} - C^*} = Mt \qquad (3.5)$$

A plot of $\ln \frac{C_{1(0)} - C^*}{C_{1(t)} - C^*}$ vs. t will yield a linear plot with slope M, where

$$M = \frac{Q_w}{V_w}\left[e^{(-KA/Q_w)} - 1 \right]$$

From the slope of equation (3.5),K can be calculated:

$$K = -\frac{Q_w}{A}\left[1 + \frac{V_w}{Q_w} M \right] \qquad (3.6)$$

3.1.3 Absorption of oxygen with membrane module immersed in a tank.

A completely mixed reactor with a membrane module immersed and gas in dead end mode, oxygen diffuses through the membrane and dissolved oxygen is monitored in the reactor with time. The overall mass transfer coefficient is then calculated from the DO versus time data.

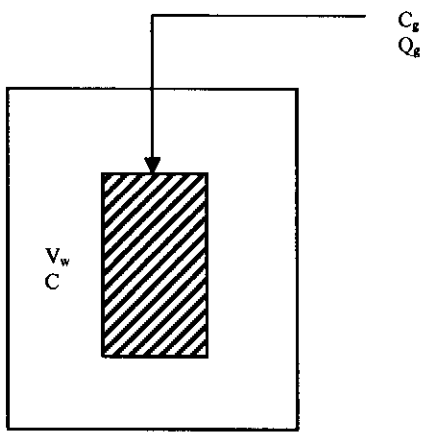

Figure 3.2: Schematic representation of oxygen absorption, with membrane immersed in a tank.

Material balance on dissolved oxygen in the tank.

Accumulation =Flow in – Flow out + Absorption

$$V_w \frac{dC}{dt} = KA(C^* - C)$$

$$V_w \frac{dC}{dt} = -KA(C - C^*)$$

Integrating the above expression from $C=C_{(0)}$ to $C= C_{C(t)}$ and t=0 and t=t yields:

$$\int_{C_0}^{C_t} \frac{dC}{C - C^*} = -\frac{KA}{V_w} \int_0^t dt$$

$$\ln \frac{C_0 - C^*}{C_t - C^*} = \frac{KA}{V_w} t \qquad (3.7)$$

A plot of $\ln \frac{C_0 - C^*}{C_t - C^*}$ vs t will yield a linear plot with slope R, where

$$R = K \frac{A}{V_w}$$

From the slope K can then be calculated

$$K = R \frac{V_w}{A} \qquad (3.8)$$

Chapter 4

EXPERIMENTAL

4.1 Introduction

To provide a design tool that is useful in the development of full-scale membrane aerator, it is convenient to use the overall mass transfer coefficient to determine the performance of the membrane in a particular reactor. For practical applications with a specific membrane type, this is most useful because it is the overall mass transfer coefficient that governs the rate of oxygen transfer. However, membrane resistances can vary for each membrane type. Thus in an attempt to make experimental results applicable to different membranes, values typically reported in literature are determined by considering only the liquid side mass transfer coefficient k_L.

As discussed previously, the overall resistance to mass transfer is composed of a gas phase resistance, membrane resistance and a liquid phase boundary layer resistance in series. In terms of mass transfer coefficients for a membrane such as silicone rubber, these factors are given as

$$\frac{1}{K} = \frac{1}{k_L} + \frac{1}{Hk_M} + \frac{1}{Hk_G} \qquad (4.1)$$

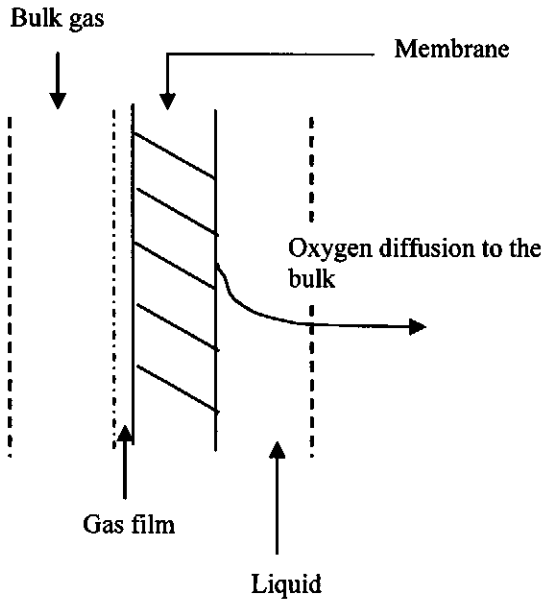

Figure 4.1: Schematic diagram of three resistances in series on overall mass transfer coefficient

where K = overall mass transfer coefficient; k_L = liquid phase mass transfer coefficient; k_M = membrane mass transfer coefficient ; k_G = gas phase mass transfer coefficient and H = Henry's law constant for oxygen and water.

The main objectives for the experiments were to determine the overall mass transfer coefficient at different operating conditions (oxygen supply pressure, liquid upflow velocity, temperature) and membrane geometry within the reactor, axial arrangement of the membranes vs transverse).

4.2 Materials and method

4.2.1 Membranes

Membranes were made up using silicone rubber from two different suppliers. It was found that the different batches of silicone rubber had no significant effect on the permeability of the membrane.

4.2.2 Apparatus

4.2.2.1 Oxygenation system

The equipment includes a 30 L rectangular Perspex tank, a dissolved oxygen (DO) meter (Hanna HI 9143), and a rectangular stainless steel membrane manifold (Figure 4.1). Mixing was achieved by using a centrifugal pump with a capacity of $2m^3/h$

Oxygen was supplied to the membranes from an oxygen cylinder controlled by a regulator. Dissolved oxygen was measured in the tank using a DO probe.

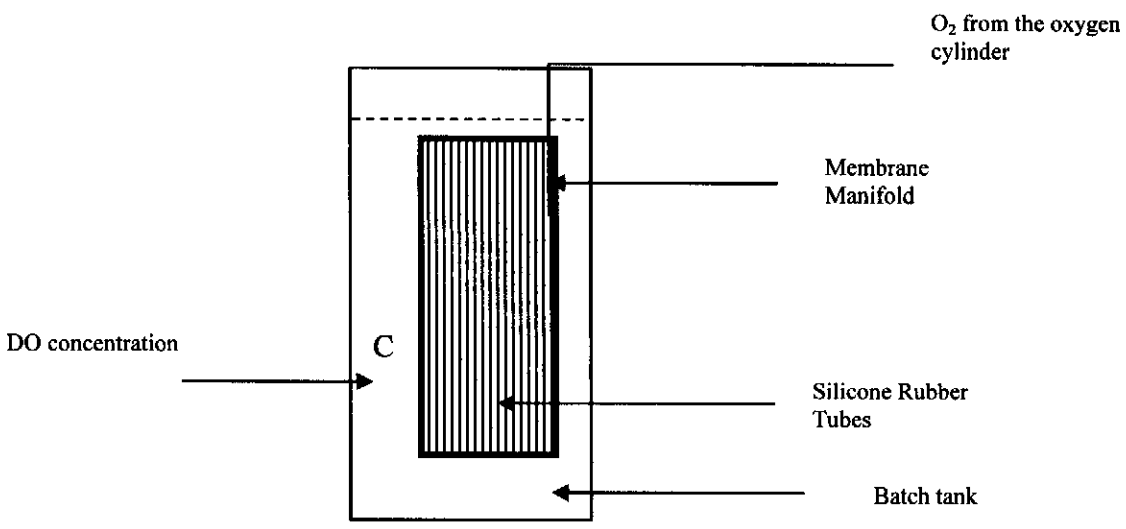

Figure 4.2 Schematic for experimental set-up

4.2.2.2 Difficulties experienced in developing the experimental system

Initially the reactor had an active volume of 25 L, and there was about 5 L of empty space. The 5 L dead zone caused some oxygen to diffuse to the air filled zone. Also the reactor was not air tight because of the mixers. An experiment to quantify these losses was done and it seemed that a reasonable amount of oxygen was lost to atmosphere. The results are shown in figures Figure 4.3 and Figure 4.4

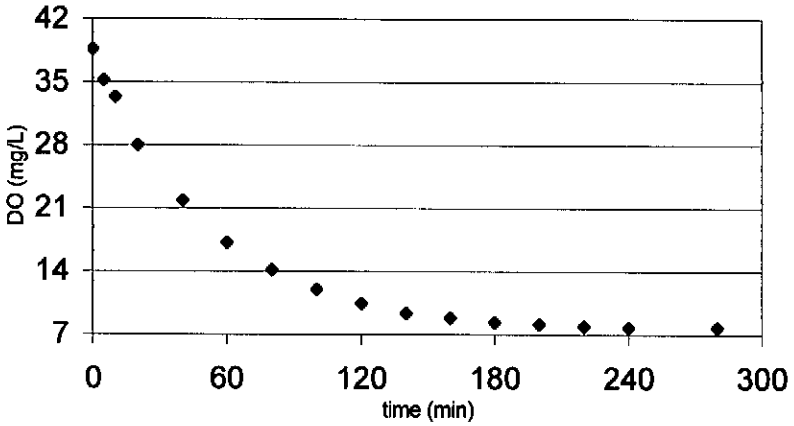

Figure 4.3. The rate at which oxygen escapes the reactor.

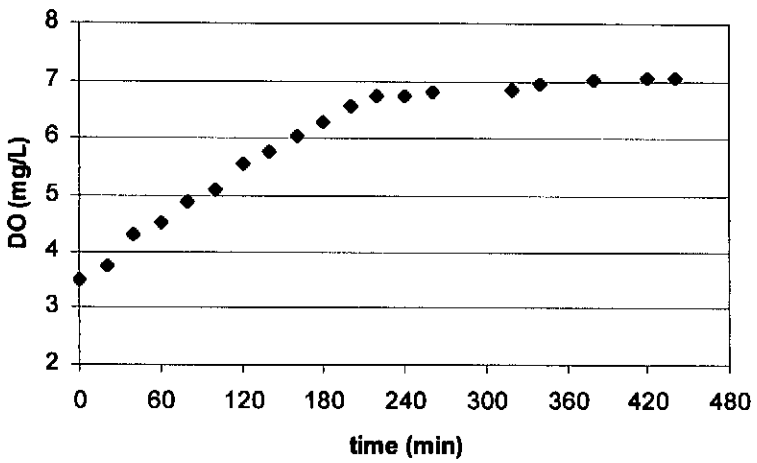

Figure 4.4. The rate at which water absorbs oxygen from the surrounding air

Pure oxygen was bubbled through the reactor to a DO concentration of about 39 mg/L. Water was continuously stirred for a period of 300 minutes. From this it then showed that a significant amount of oxygen was lost to the atmosphere. Also an experiment where sodium sulphite was used to deplete oxygen in water was carried out and the DO was monitored with time (Figure 4.4). The results show that oxygen was absorbed from the atmosphere up until water was in equilibrium with air at about 7 mg/L.

4.2.2.3 Modified experimental system

As a result of the difficulties presented in section 4.2.22, a modified experimental system as shown in Figure 4.5 was developed. The reactor was operated at 100% volume. It was coupled with a funnel at the top for easy filling of the reactor with water also as a pressure relief for any build-up of pressure. Also a liquid flow distributor was installed for improved mixing. This modified set-up seemed to have solved the problems encountered during the developmental stage of the experimental system (Figure 4.8 to Figure 4.11).

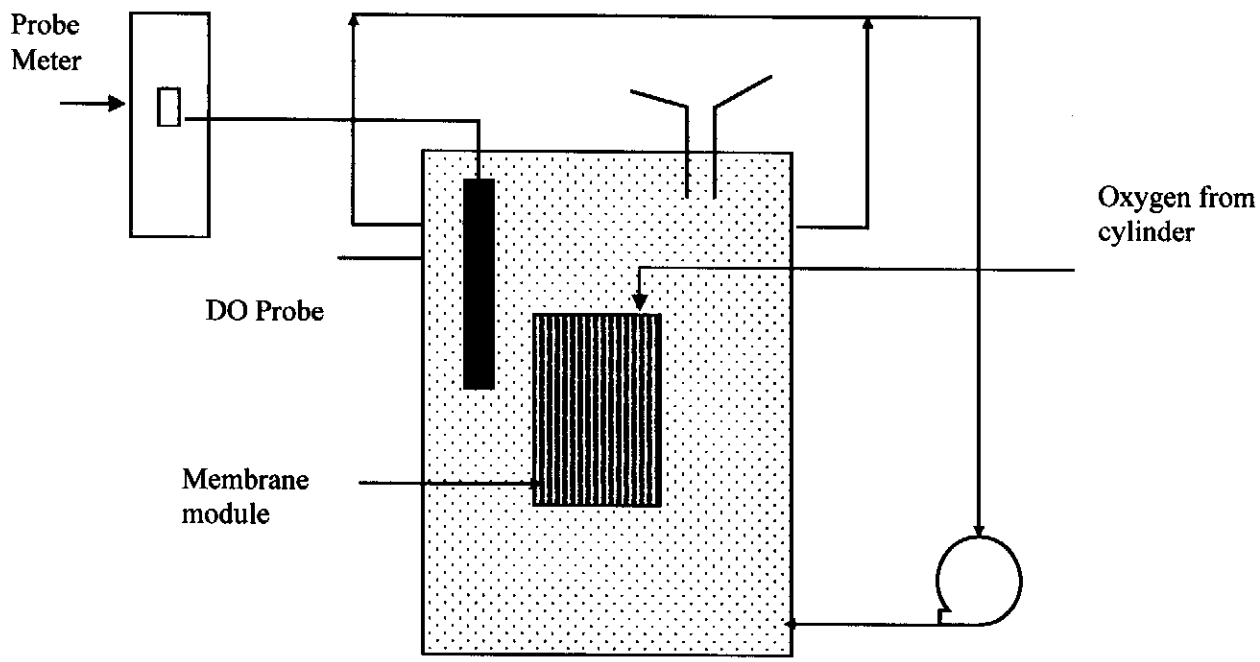

Figure 4.5 Schematic for a modified experimental set-up

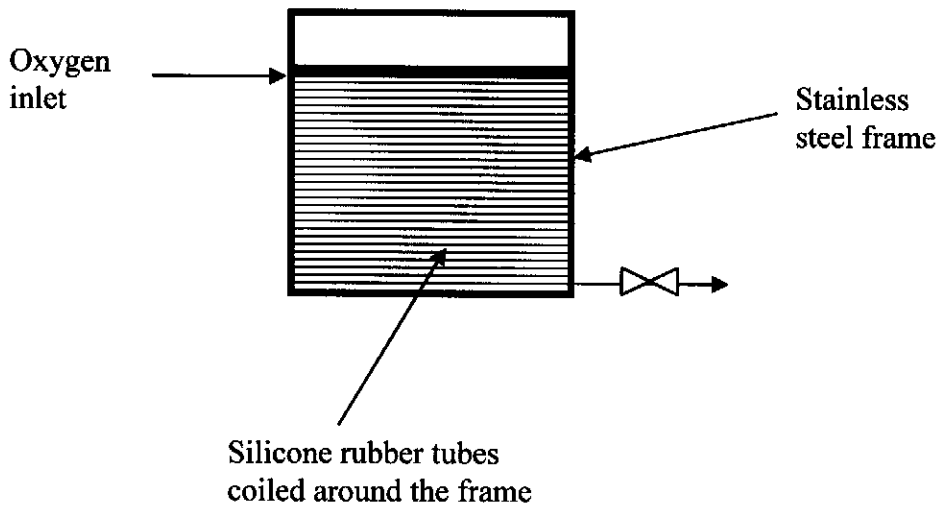

Figure 4.6 Schematic of a single membrane manifold

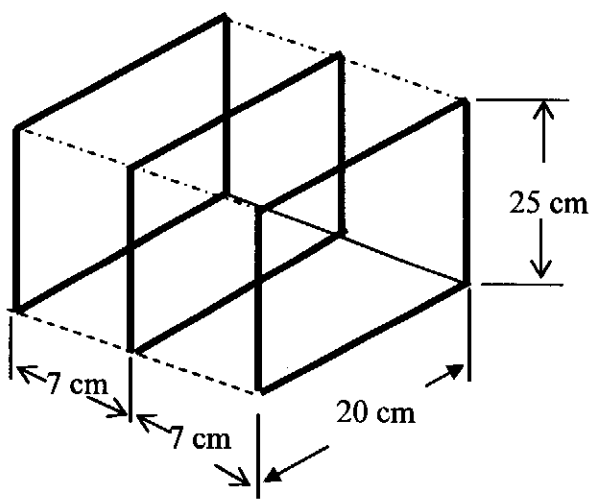

Figure 4.7 Schematic of three frames making the overall manifolding system

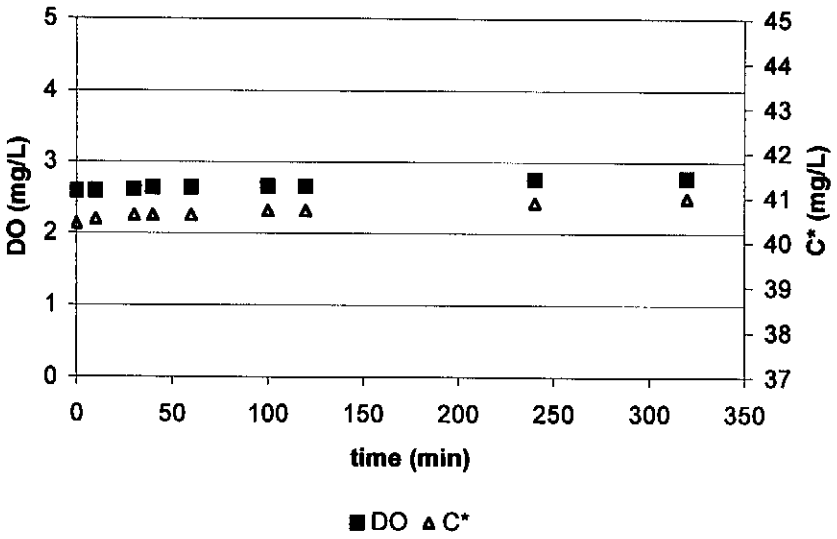

Figure 4.8 Dissolved oxygen and saturation concentration profile with time below the equilibrium concentration

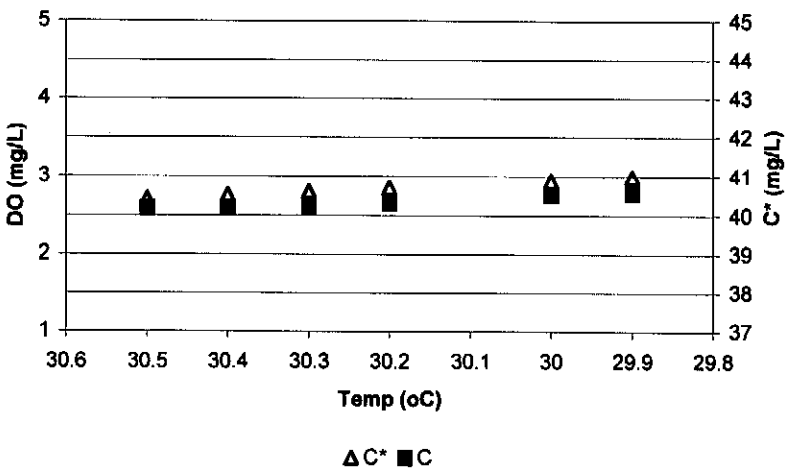

Figure 4.9 Dissolved oxygen and saturation concentration profile with temperature below equilibrium concentration

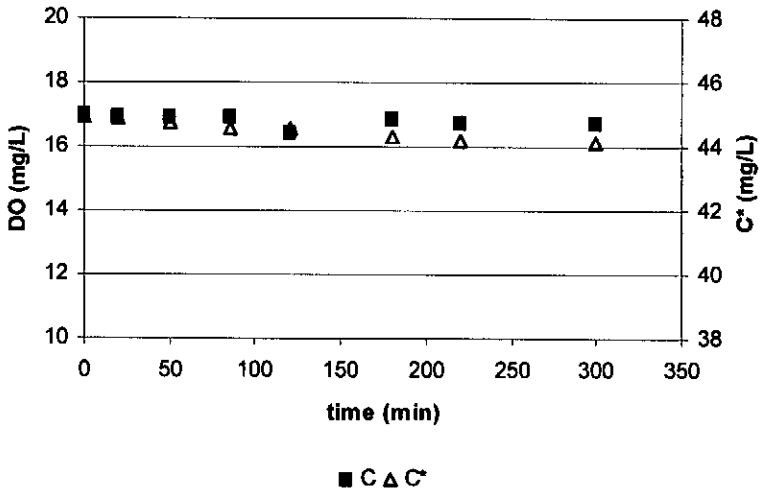

Figure 4.10 Dissolved oxygen and saturation concentration profile with time above the equilibrium concentration

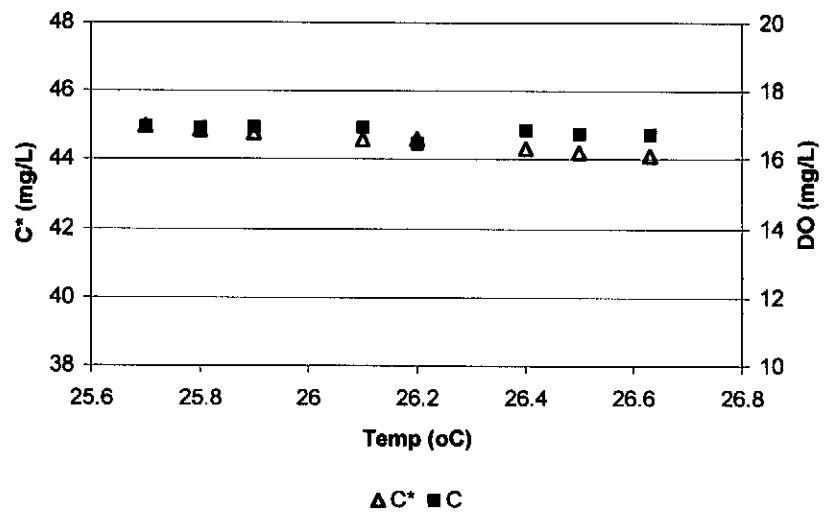

Figure 4.11 Dissolved oxygen and saturation concentration profile with temperature above the equilibrium concentration

4.2.3 Operation Process

4.2.3.1 Calibration of DO Probe

Calibration of DO probe is necessary for precise measurement. The methods used in this study consist of zero check and saturation check. The zero check is run every time the probe is switched on, by putting the probe into a zero DO solution, which is achieved by dissolving sodium sulphite in water. Saturation check can be done anytime before the start of the experiment or after completion of the experiment.

4.2.3.2 Temperature Measurements

The temperature of the test water can also be read from the DO meter. The DO meter has a temperature sensor built onto the probe. The temperature can be measured to an accuracy of ± 0.2 °C.

4.2.3.3 Oxygen flow rate Measurements

A laboratory flowmeter with a maximum flow of 92 mL/min was used to measure oxygen flow rate. The accuracy of the flowmeter was checked before use. An inverse measuring cylinder filled with water was used to calibrate oxygen flow rate.

4.3 Methodology

Pure oxygen was fed from an oxygen cylinder by a pressure regulator valve through the membrane module. Oxygen diffuses through the membrane into the water. All the experiments were carried out at ambient temperature (25 °C and atmospheric pressure). The DO concentration of fresh water was lowered to 2-3 mg/L by addition of sodium sulphite with a cobalt catalyst. DO was recorded as a function of time as shown in Figure 4.12

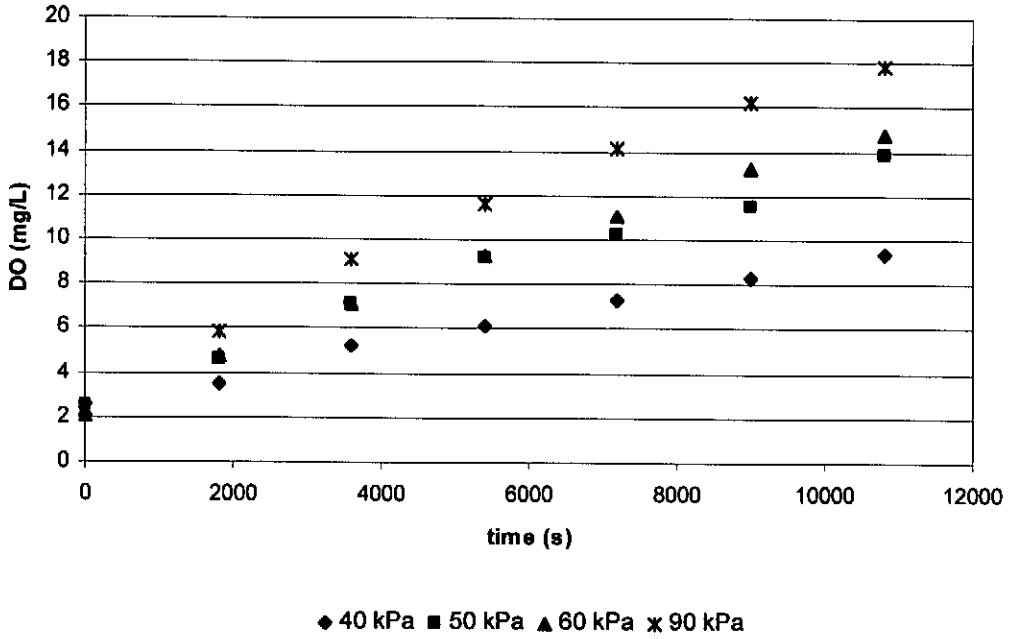

Figure 4.12: Effect of pressure and time of oxygen on the DO conentration

The data collected from experiments was used to calculate the overall mass transfer coefficient (K). A typical plot of data collected from experiments is shown in figure 4.12 A linear regression method is used to analyse data from the experiment. This method is based on the model through the DO-versus-time data. The increase in DO is given by the following equation:

$$C_t = C^* - (C^* - C_0) * \exp(-\frac{KA}{V}t) \qquad (4.1)$$

Where C_t = DO concentration at any time t

C^* = Equilibrium DO concentration

C_0 = Initial DO concentration

K = Overall mass transfer coefficient

V = Active volume of the reactor

t = time

However, equation (4.1) gives a non- linear relationship between DO concentration and time. Transformation of this equation is necessary before it is applied. A linear relationship can be obtained by equation (4.2).

$$\ln\frac{C_0 - C^*}{C_t - C^*} = \frac{KA}{V_w}t \qquad (4.2)$$

A plot of $LnY = \ln\left(\frac{C_0 - C^*}{C_t - C^*}\right)$ versus time is a straight line as shown in Figure 4.13. The slope of the straight line which is the quantity $\frac{KA}{V_w}$ is determined and the value of the mass transfer coefficient K is calculated.

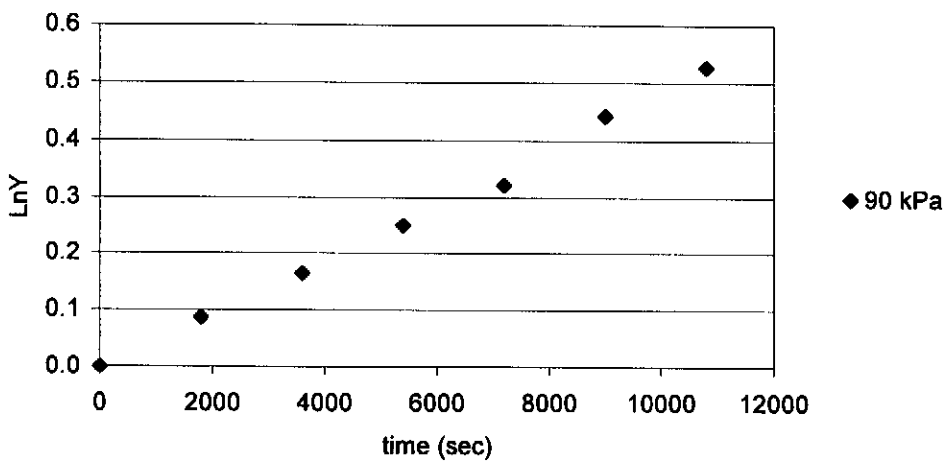

Figure 4.13. A plot of LnY vs time

Chapter 5

RESULTS AND DISCUSSION

---

5. Results

5.1 Introduction

The objective of the study was to evaluate the use of silicone rubber membranes as a means of providing oxygen into bioreactors. A reactor operated on water was set-up to determine mass transfer rates through silicone rubber. Experiments conducted were to determine the effect of oxygen supply pressure on mass transfer, effect of cross flow velocity of water on mass transfer, effect of membrane positioning within the reactor (axial vs. transverse) and the effect of temperature.

All the experiments were done below equilibrium dissolved oxygen concentration due to the fact that typical membrane bioreactors operate at about 4 mg/l-dissolved oxygen. Cross flow velocity of water was determined at three different flow rates (2000 L/h, 1500 L/h and 1000 L/h). Below a flow rate of 1000 L/h uniform concentration could not be achieved within the reactor, making it difficult to monitor dissolved oxygen.

Initial experiments were done to determine oxygen permeability of the membrane before mass transfer experiments were done. In line with literature, silicone rubber did show better oxygen permeability than most polymers. Yasunda and Lamaze, (1972) studied oxygen permeability using different membranes ranging from porous membranes coated with a thin layer of silicone to non-porous silicone rubber. Silicone rubber did show better permeabilities both on gas-membrane-gas and gas-membrane-water systems.

5.2 Reproducibility of the measurements

Repeatability on the data collected was very good. Figure 5.1 and 5.2 show the repeated measurements for the data collected to calculate overall mass transfer coefficients. The relative deviation from the mean value ranged between 2 and 4%.

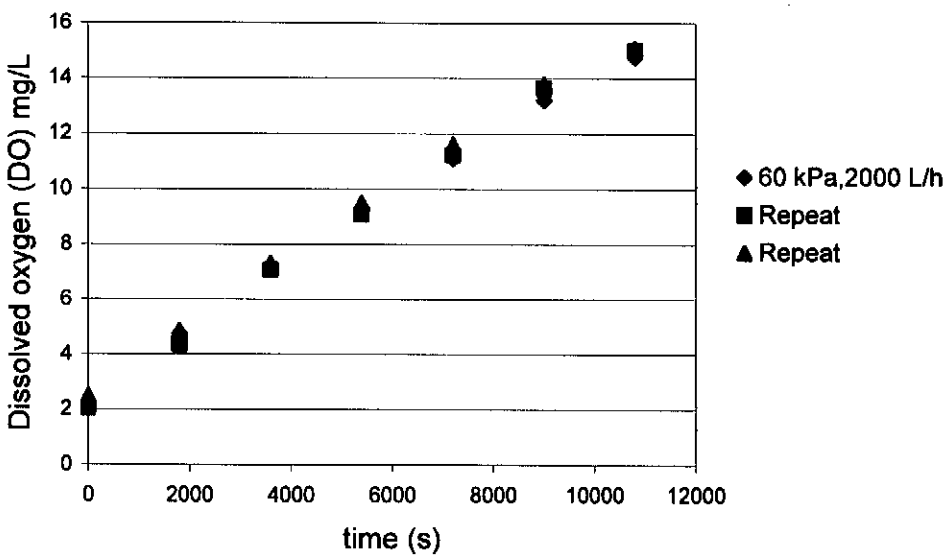

Figure 5.1. The dissolved oxygen profile with time at 2000 L/h

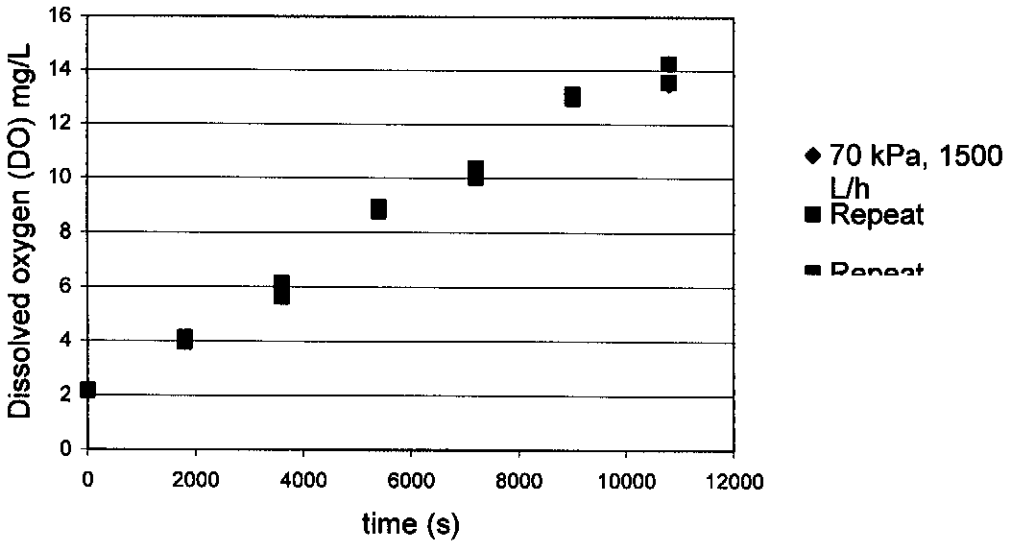

Figure 5.2. The dissolved oxygen profile with time at 1500 L/h

5.3 Kinetics of membrane aeration

The change in dissolved oxygen within the reactor followed the proposed kinetics; that is, for the plot of lnY versus time, a straight line was obtained. The development of a lnY relationship is referenced in chapter 3. Figure 5.1 shows the plots resulting from a series of experiments performed at varying flow rates. The strong influence of hydrodynamic conditions on oxygen mass transfer can be seen from different slopes of the curves.

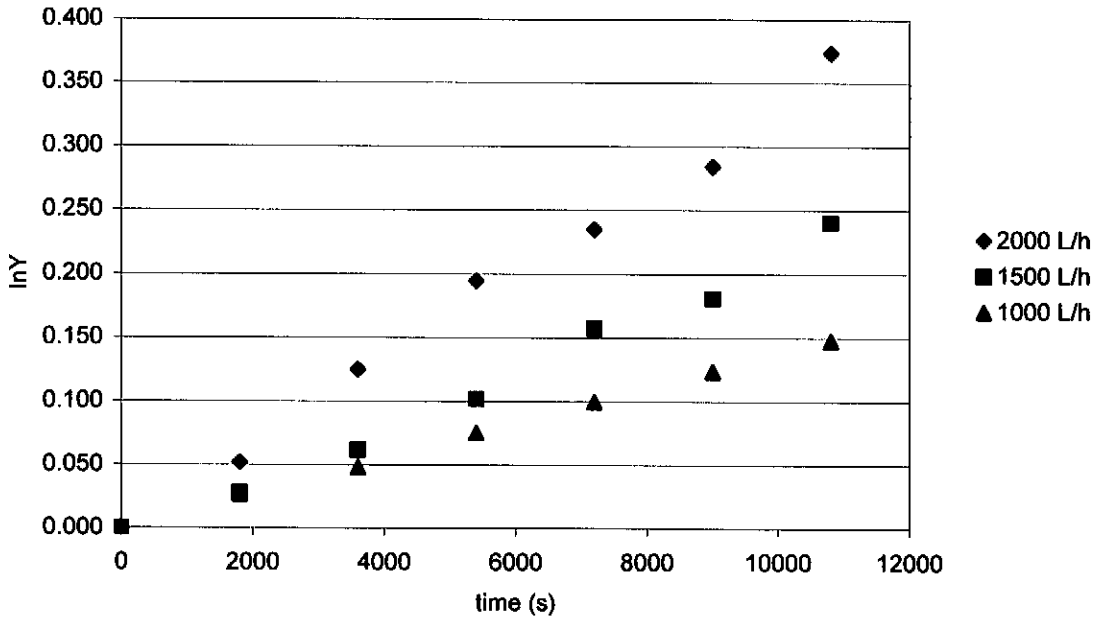

Figure 5.3. The transformed response of the dissolved oxygen probe versus time for the different flow rates.

5.4 Effect of oxygen supply pressure on mass transfer

Figure 5.4 shows the overall mass transfer coefficient with pressure. There seem to be an increase in overall mass transfer coefficient with increasing pressure up to 90 kPa where there is no significant difference on overall mass transfer coefficient with increasing liquid flow rate.

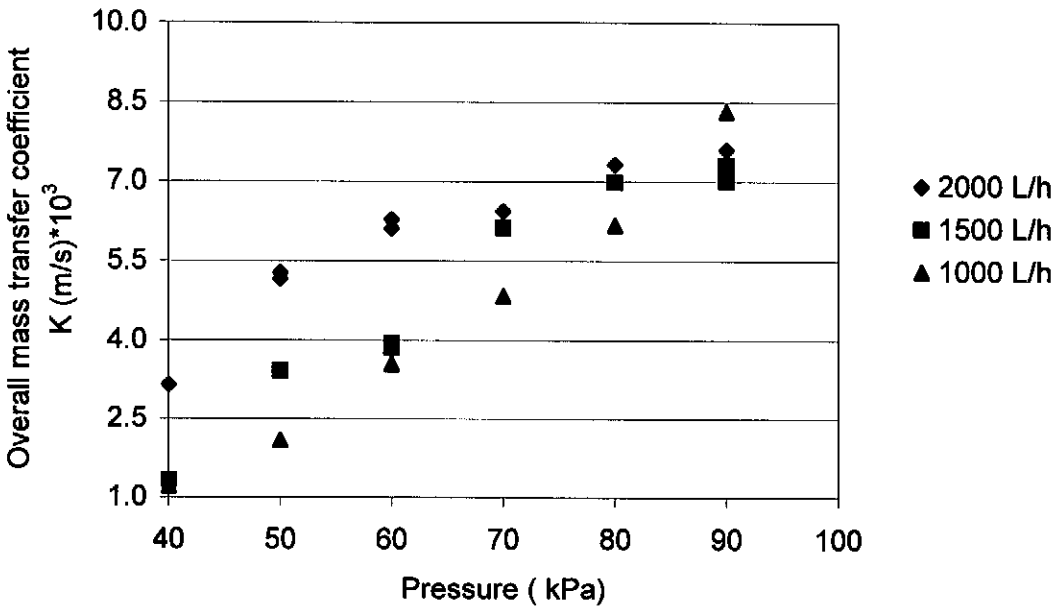

Figure 5.4. Overall mass transfer coefficient (K) with pressure at different cross f low velocities

The observed results can be described by the following theories. Transport of gas through the membrane is a pressure driven process. From chapter 4 the theory of gas permeation is discussed and equations that describe the process are given. The combination of Henry's law, Eq (5.1) and Fick's Eq law (5.2) yields an oxygen flux equation (5.3), which uses pressure difference as a driving force.

$$C = k_D p \tag{5.1}$$

$$J = -D\frac{\delta C}{\delta x} \tag{5.2}$$

$$J = \frac{k_D D \Delta p}{\ell} = P\frac{\Delta p}{\ell} \tag{5.3}$$

where C is the oxygen concentration in the membrane, D is the diffusion coefficient of oxygen in water, k_D is the absorption coefficient and Δp is the pressure difference between the inside and the outside of the membrane. P is the steady state permeability.

Equation 5.3 shows that oxygen flux through the membrane is a function of pressure, up to a certain level. After which the system is no longer controlled by pressure. This is evident in Figure 5.4 where at 90 kPa there seem to be no change in overall mass transfer coefficient.

The general approach to determine the overall mass transfer coefficient is to look at all the resistances that play part in the mass transfer process through the membrane. The overall resistance to mass transfer is composed of three resistances, a gas phase resistance, membrane resistance and a liquid phase boundary layer resistance in series. In terms of mass transfer coefficients for a membrane such as silicone rubber, these factors are given as

$$\frac{1}{K} = \frac{1}{k_L} + \frac{1}{Hk_m} + \frac{1}{Hk_G} \tag{5.4}$$

The effects of pressure, orientation, and cross flow are better described by the sketch below. At low pressures transport through the membrane is purely diffusion and that is largely controlled by pressure and the membrane diffusion coefficients. At higher pressures the liquid-membrane interface becomes saturated and requires higher cross

flows to disturb the boundary layer. Hence at this stage the major resistance to flow is the liquid phase resistance.

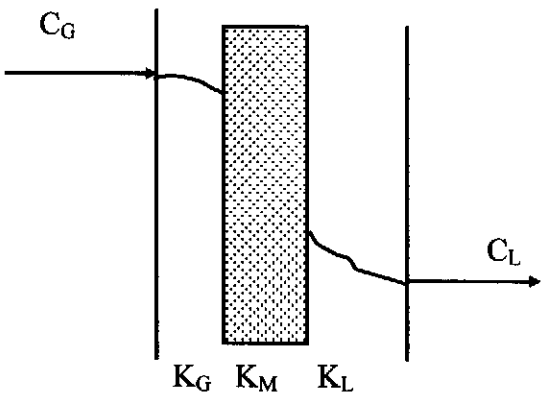

Figure 5.5. Concentration profile across the membrane interface

5.5 Effect of cross flow velocity on mass transfer

Figure 5.5 shows an increase in overall mass transfer coefficient with cross flow velocity for all pressures tested except for one pressure (80 kPa) where there is an increase at the first two-cross flow velocities and thereafter there is no significant increase in mass transfer coefficient with cross flow velocity. This can be attributed to the fact that at higher pressures there is a high oxygen flux through the membrane and the cross flow velocity might be not enough to disturb the boundary layer.

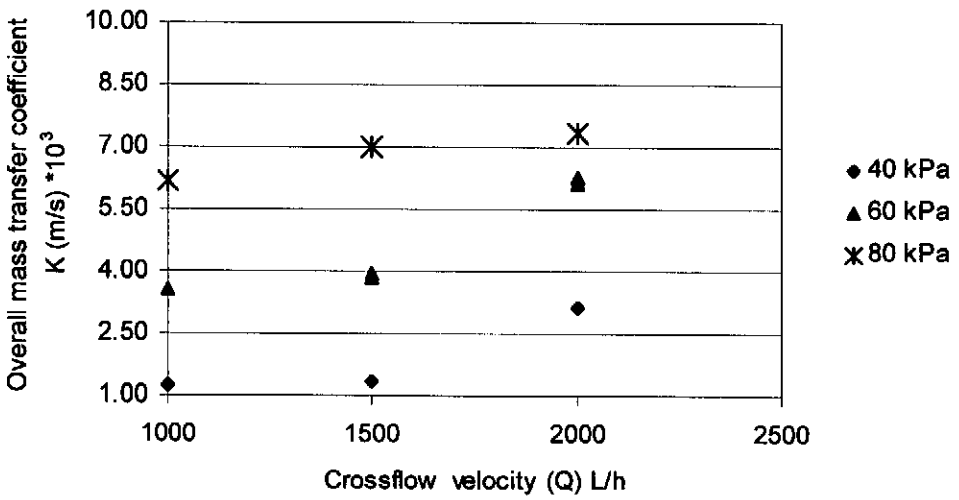

Figure 5.6 Overall mass transfer coefficient (K) with cross flow velocity at different oxygen supply pressures

Transport from the surface of the membrane to the bulk liquid is concentration dependent and is a function of hydrodynamic conditions. In mathematical form the mass transfer rate can be written as (CJ Gianakopulos, 1993)

$$m = k_L A(C^* - C) \qquad 5.5$$

where k_L is the liquid phase mass transfer coefficient, A transfer area, C* is the saturation concentration and C is dissolved oxygen concentration.

The analysis of Eq 5.5 suggests that the liquid flow rate is important when the mass transfer is controlled by the liquid film mass transfer coefficient, k_L. This condition is generally met due to the fact that oxygen has a large Henry's constant, *H*, which reduces the magnitude of the membrane and gas film resistances. Thus it is anticipated that the rate of oxygen transfer will increase as the water flow rate increases. This is evident in figure 5.5 where overall mass transfer coefficient is plotted against liquid flow rate at different oxygen supply pressures. Semmens *et al*, 1992 investigated the effect of liquid flow rate using micro porous polypropylene hollow fibres for separating volatile organic compounds (VOCs) from water. They found that the removal of VOCs increased with increasing water flow.

5.6 Effect of module orientation on mass transfer

Figure 5.7 is a plot of mass transfer coefficient versus pressure at two geometric positions, axial and transverse. From the results it can be seen that the transverse configuration has higher mass transfer coefficient than axial configuration between pressures of 50 kPa and 80 kPa. After which there is no change on mass transfer with module positioning. The trend that is noticed is that mass transfer activity is noticed between pressures of 50 kPa and 80 kPa. Mass transfer coefficient is a strong function of hydrodynamic conditions. For transverse orientation the entire length of the membrane is tangential to the direction of flow, thus the disturbance of the boundary layer is higher and hence higher mass transfer coefficients. For the Axial orientation only the cross section of the membrane is in the direction of flow such that the disturbance of the boundary layer is minimal and not effective enough to enhance mass transfer.

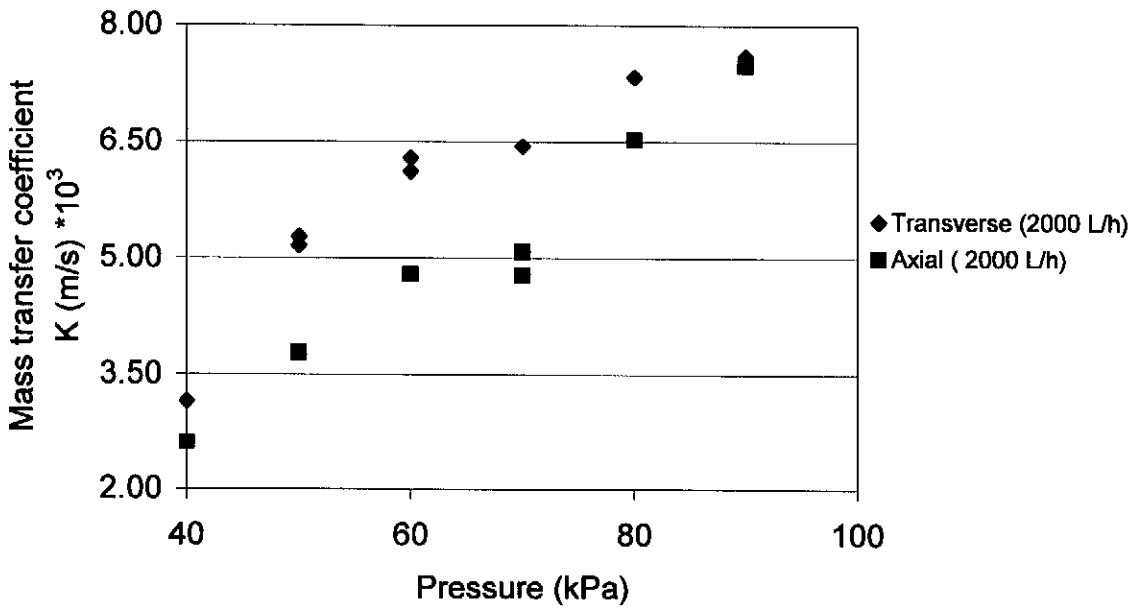

Figure 5.7 Overall mass transfer coefficient (K) with pressure at different geometric positioning at 2000 L/h cross flow

However at lower cross flow velocities there appears to be no significant difference in mass transfer coefficient with geometric orientation (Figure 5.7). This can be attributed to the cross flow velocity (1000 L/h) being too low hence not creating sufficient turbulence to effect good mixing.

As it was mentioned earlier that liquid flow rate is an important part of mass transfer. The rate at which water flows past the membrane and the direction of the membrane determines the value of mass transfer (K). More effective contact is attained if water strikes the surface of the membranes at an angle perpendicular to the direction of the membrane than if water flows parallel to the membranes, Semmens *et al*, 1992.

Figure 5.6 shows the effect of orientation and from that it can be seen that transverse orientation has better mass transfer than axial at cross flow velocity of 2000 L/h. However in Figure 5.7 for a cross flow of 1000L/h there seems to be no significant difference with axial and transverse orientation. This can be attributed to the fact that at low cross flow velocity mass transfer is only due to diffusion rather than both diffusion and convective transport.

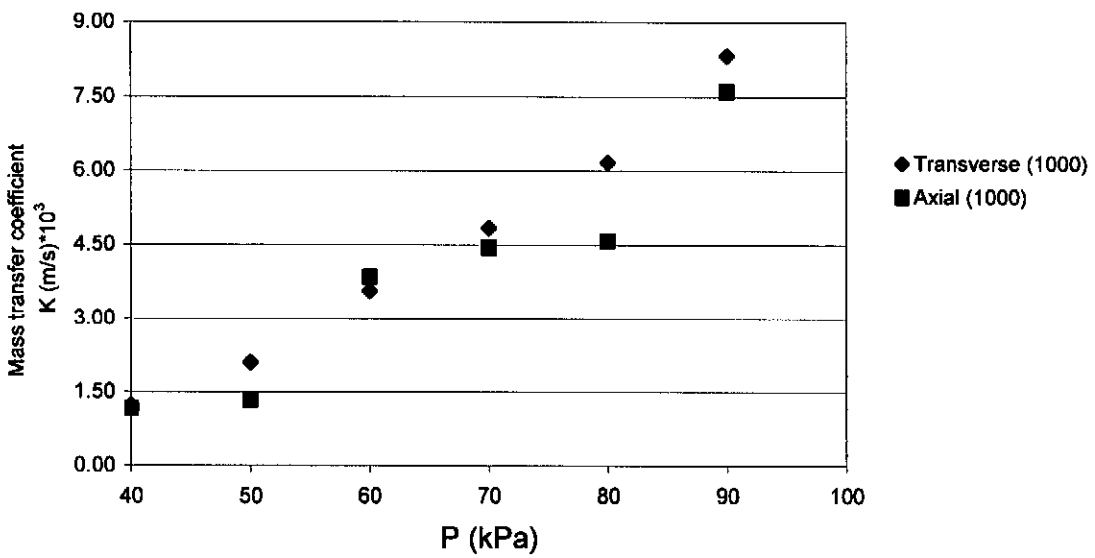

Figure 5.8 Overall mass transfer coefficient (K) with pressure at different geometric positioning at 1000 L/h cross flow

5.7 Effect of temperature on mass transfer

Figure 5.9 shows the overall mass transfer coefficient with pressure at two different temperature conditions which are ambient conditions (20°C-30 °C) and high temperature (35°C-45 °C).

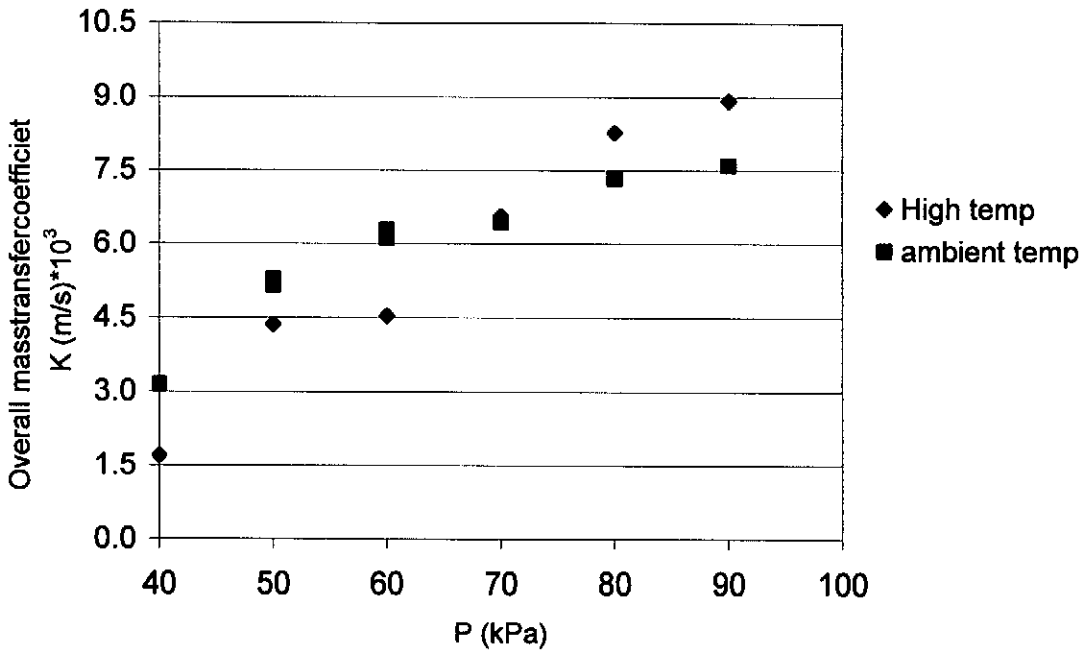

Figure 5.9 Overall mass transfer coefficient (K) with pressure At high temperature and ambient temperature conditions

The effect that the temperature has on overall mass transfer in not well known. Literature explains this effect in two different ways that somehow make it difficult to observe.

- Solubility theory

Equation 5.5 shows the driving force (C*-C). From the experiments, there as a reduction of approximately 50 % in solubility (C*) from ambient to high temperature trials. This implies a reduced driving force.

- Viscosity theory

At high temperature the viscosity of water decreases and that reduces the liquid boundary layer resistance. If one considers the relationship of Sherwood number and Reynolds number, Sherwood number has a mass transfer component in it and Reynolds has a viscosity component, and the relationship can be written as

$$Sh = f(\mathrm{Re}, Sch)$$

Where $\mathrm{Re} = \frac{\rho dv}{\mu}$, $Sh = \frac{kL}{D}$ and $Sch = \frac{\gamma}{D}$.

From this relationship increasing Reynolds by decreasing viscosity should increase mass transfer coefficient.

It can be concluded that the effects might have counter acting effect on overall mass transfer coefficient.

5.8 Summary

The effects of pressure, cross flow velocity, module orientation and temperature were evaluated at pressures ranging from 40 kPa to 90 kPa and three cross flow velocities of 100 L/h, 1500 L/h and 2000 L/h. All the results except the effect of temperature followed the three resistances in series model (equation 5.4), where at low pressures oxygen transport is controlled by diffusion and at high pressures it is controlled by the liquid phase resistance.

The effect of cross flow velocity on overall mass transfer coefficient was seen to have a significant on effect overall mass transfer coefficient. However at higher pressure (90 kPa); the liquid flow rates chosen were not enough to disturb the boundary layer. This meant that transport from the surface of the membrane to the bulk liquid was restricted.

Module orientation showed that transverse configuration yields better mass transfer coefficient than axial configuration.

The effect of temperature did not show a significant difference on overall mass transfer coefficient for the two temperature ranges tested. This is not a well understood phenomenon due to the counter effect of oxygen solubility decreasing at high temperature and viscosity decreasing.

Chapter 6

CONCLUSIONS AND RECOMENDATIONS

This study has concerned the characterisation of an immersed aerated membrane bioreactor. This was done by investigating the effects of oxygen supply pressure, liquid crossflow velocity, module orientation, and effect of temperature to compare the performance of the membranes at both thermophilic and mesophilic conditions. A mathematical model was then developed to experimentally determine mass transfer coefficients.

Clean water was used as a test fluid so as to eliminate the complexities of a biological suspension. This gives the mass transfer characteristics of silicone rubber membrane without any fouling of the membrane.

From the results it is evident that mass transfer coefficient is a strong function of system hydrodynamic conditions. For those runs with crossflow velocity of 2000 L/h the system was controlled by the concentration gradient from the membrane surface to the bulk liquid, and at crossflow velocity of 1000 L/h the system was controlled by pressure. It was then evident that, to achieve good mass transfer the system hydrodynamic conditions need to improve. With the kind of manifolding system developed in this study, a vibrating mechanism on the module frame can improve the disturbance of the boundary layer and hence improve mass transfer rate from the membrane surface to the bulk.

The design of the manifolding system was done in such a way that flat sheet membranes can be placed in-between silicone rubber tubes for direct oxygen delivery. From the

results it was noticed in order to achieve better mass transfer results, the membranes cannot be run for longer periods as some kind of vapour forms on the lumen side of the tubes. This then caused some kind of resistance and results in poor mass transfer coefficients. This was proved buy leaving the membrane immersed in water over night. It is recommended that one set of silicone rubber aerators be run in a bioreactor for not more that eight hours. It can be replace buy a clean one the other one cleaned and allowed to dry so that any vapour that would have accumulated on the inside would dry out.

The overall mass transfer coefficient is affected by a combination of all the factors discussed in the study. But if one looks at individual mass transfer coefficients some of the factors do not affect the process. Liquid phase mass transfer coefficient is affected by the crossflow velocity. Oxygen supply pressure only affects the oxygen flux through the membrane. Module orientation has a significant effect on mass transfer, transverse orientation showed better mass transfer results than axial. The effect of temperature is a bit complex, there is a significant difference in oxygen uptake rate but it is not that clear if one looks at mass transfer coefficient.

References

1. Pankhania M, Brindle K, Stephenson T, Membrane aeration bioreactors for wastewater treatment: completely mixed and plug-flow operation, Chemical *Engineering Journal*, 73 (1999), 131-136

2. Ahmed T, Semmens MJ, Use of sealed end hollow fiber for bubble less membrane aeration: experimental studies, *Journal of Membrane Science*, 69 (1992) 1-10

3. Ahmed T, Semmens MJ, Use of transverse flow hollow fiber for bubble less membrane aeration, *Journal of Membrane Science*, 30 (1996) 440-446

4. Ahmed T, Semmens MJ, The use of independently sealed micro porous hollow fibre membranes for oxygenation of water: model development, *Journal of Membrane Science*, 69 (1992) 11-20

5. Brindle K, Stephenson T, Semmes MJ, Nitrification and oxygen utilization in a membrane aeration bioreactor, *Journal of Membrane Science*, 144 (1998), 197-209

6. Casey E, Glennon B, Hamer G, Review of membrane aerated biofilm reactors, Conservation *and Recycling*, 27 (1999), 203-215

7. Casey E, Glennon B, Hamer G, Oxygen mass transfer characteristics in a membrane-aerated biofilm reactor, *Biotechnology and bioengineering*, 62 (1999), 183-192

8. Coulsen JM, Richardson JF, *Chemical Engineering*, Volume 2, 4th edition, Pergamon Press, 1991

9. Côté P, Bersillon J-L, Huyard A, Bubble free aeration using membranes: Process analysis, *Journal of Membrane Science*, 60 (1988), 1986-1992

10. Côté P, Bersillon J-L, Huyard A, Bubble free aeration using membranes: Mass transfer analysis, *Journal of Membrane Science*, 47 (1989), 91-106

11. Demoyer CD, Schierhols EL, Gulliver JS, Wilhelms SC, Impact of bubble and free surface oxygen transfer on diffused aeration systems, *Water Research*, 37 (2003), 1890-1904

12. Essila NJ, Semmens ML, Voller VR, Modeling biofilms on gas-permeable supports: concentration and activity profiles, *Journal of Environmental Engineering*, 126(3) (2000) 250-257

13. Geankoplis CJ, *Transport processes and unit operations*, 3rd edition, Prentice hall, 1993

14. He Z, Petiraksakul A, Meesapya W, Oxygen –transfer measurements in clean water, *Journal of King Mongkut's Institute of Technology North Bangkok*, 13 (2003), 14-19

15. Ito A, Yamagiwa K, Tamura M, Furusawa M, Removal of dissolved oxygen using non-porous hollow-fiber membranes, *Journal of Membrane Science*, 145 (1998), 111-117

16. Kinnan CM, Jonson DW, Iron fouling in membrane gas transfer applications, *Journal of Membrane Science*, 5272 (2002), 1-27

17. Metcalf and Eddy, Wastewater Engineering: treatment, disposal and reuse, 3rd edition, McGraw Hill, New York, 1991

18. Moulin P, Rouch JC, Serra C, Clifton MJ, Aptel A, Mass transfer improvement by secondary flows: dean vortices in coiled tubular membranes, *Journal of Membrane Science* 114 (1996) 235-244

19. Perry RH and Green DW, Chemical Engineer's Handbook, 6th edition, McGraw-Hill, New York, 1984

20. Qi Z, Cussler EL, Micro porous hollow fibers for gas absorption I. Mass transfer in the liquid, *Journal of Membrane Science*, 23 (1985), 321-332

21. Schneider M, Reymond F, Marison IW, von Stockar U, Bubble free oxygenation by means of hydrophobic porous membranes, *Enzyme and Microbial Technology*, 17 (1995), 839-847

22. Schnabelm S, Moulin P, Nguyen QT, Roizard D, Aptel P, Removal of volatile organic components (VOC) from water by pervaporation: separation improvement by Dean vortices, *Journal of Membrane Science,* 142 (1998), 129-141

23. Schaffer RB, Ludzack FJ, Ettinger MB, Sewage treatment by oxygenation through permeable plastic films, *Journal of the Water Pollution Control Federation*, 32 (9) (1960) 939-941

24. Semmens MJ, K Dahm, Shanahan J, Christianson A, COD and nitrogen removal by biofilms growing on gas permeable membranes, *Water Research*, 37 (2003), 4343-4350

25. Semmens MJ, Qin R, Zander A, Using a micro porous hollow fiber membrane to separate VOCs from water, *American Water Works Association Journal*, 81 (4) (1989), 162-167

26. Treybal RE, *Mass Transfer Operations*, 3rd edition, McGraw-Hill, New York, 1980

27. Van de Valt A, (1999), Design and characterization of transverse flow module for gas transfer operation. MSc Thesis, University of Stellenbosch

28. Vladisavljević GT, Use of polysulphone hollow fibers for bubble less membrane oxygenation/deoxygenating of water, *Separation and Purification Technology*, 17 (1999), 1-110

29. Wiss PT, JS Gulliver, Semmens MJ, In-stream hollow fiber membrane aeration, *Journal of Hydraulic Engineering*, 124(6) (1998) 579-588

30. Wijmans JG, Baker RW, The solution diffusion model: a review, *Journal of Membrane Science*, 107 (1995), 1-21

31. Yeh SJ, Jenkins CR, Pure oxygen fixed film reactor, *Journal of The Environmental Engineering Division*, (1978), 611-623

32. Yasunda H, Lamaze CE, Transfer of gas to dissolved oxygen in water via porous and nonporous membranes, *Journal of Applied Polymer Science*, 16 (1972) 596-601

33. Yang MC and Cussler EL, Designing hollow-fiber contactors, *AIChE Journal*, 2(1986) 1910-1916

APPENDICES

APPENDIX A

Conversion factors for Henry's constant

Henry's constant is usually defined as

$$H_x = \frac{P}{x}[atm/molefraction]$$

where

P = partial pressure of solute gas [atm]

X = mole fraction of solute in the liquid phase [mole fraction]

The following values for Henry's constant are obtained from literature for oxygen at different temperatures:

T (°C)	H_x (atm/mol frac)
0	2.55E+04
10	3.27E+04
20	4.01E+04
30	4.75E+04
40	5.35E+04

Conversion from H_x to H_p can easily be done:

$$H_p = \frac{P}{C_L} = H_x.\upsilon_s[atm..m^3/mol]$$

where:

C_L = concentration of solute in the liquid phase [mol/m^3] or [mg/L]

υ_s = molar volume of aqueous solution [m3/mol]

= 1.8E-5 m^3/mol for water

Values for Henry's constant with various units:

T (°C)	H_x (atm/mol frac)	H_p (atm.m^3/mol)	H_p (kPa. L/mg)
0	2.55E+04	0.479	1.498
10	3.27E+04	0.615	1.921
20	4.01E+04	0.754	2.356
30	4.75E+04	0.893	2.791
40	5.35E+04	1.006	3.143

References

JM Coulsen, JF Richardson, *Chemical Engineering*, Volume 2, 4th edition, Pergamon Press, 1991

CJ Geankoplis, *Transport processes and unit operations*, 3rd edition, Prentice hall, 1993

R.H. Perry and D.W. Green, *Chemical Engineer's Handbook*, 6th edition, McGraw-Hill, New York, 1984.

APPENDIX B
EXPERIMENTAL RESULTS

Q **2000 L/h**

PG **30** **kPa**
Area **0.2279** **m2**

time (sec)	DO (mg/L)	Temp (oC)	C* (mg/L)	LnY
0	2.01	21	44.72	0
1800	2.5	23.2	44	0.0200
3600	2.98	25.9	42.01	0.0342
5400	3.2	28.5	40.84	0.0493
7200	4.36	29.3	39.93	0.0626
9000	4.7	30.1	38.85	0.0794
10800	5.12	32	38.13	0.0926
Slope	8.43E-06			
K (m/s)	**1.29E-03**			

Q **2000 L/h**

PG **40** **kPa**
Area **0.2279** **m2**

time (sec)	DO (mg/L)	Temp (oC)	C* (mg/L)	LnY
0	2.08	23.4	45	0
1800	3.55	25	43.55	0.0361
3600	5.22	27	41.74	0.0825
5400	6.11	27.7	41.11	0.1090
7200	7.3	28.9	40.02	0.1480
9000	8.3	29.9	39.12	0.1838
10800	9.37	30.8	38.3	0.2247
Slope	2.05E-05			
K (m/s)	**3.15E-03**			

Q **2000 L/h**

PG **50** **kPa**
Area **0.2279** **m2**

time (sec)	DO (mg/L)	Temp (oC)	C* (mg/L)	LnY
0	2.5	25	43.54	0
1800	4.55	25.6	43	0.0519
3600	7.09	27.1	41.65	0.1247
5400	9.18	28.6	40.3	0.1945
7200	10.26	29.4	39.57	0.2349
9000	11.56	29.9	39.12	0.2842
10800	13.89	30.6	39.03	0.3737
Slope	3.36E-05			
K (m/s)	**5.16E-03**			

Q **2000 L/h**

PG **60** **kPa**
Area **0.2279** **m2**

time (sec)	DO (mg/L)	Temp (oC)	C* (mg/L)	LnY
0	2.1	23.6	44.81	0
1800	4.75	25.2	43.37	0.0664
3600	7.1	26.6	42.1	0.1335
5400	9.3	28	40.84	0.2056
7200	11.1	28.9	40.02	0.2709
9000	13.2	30	39.03	0.3575
10800	14.76	30.7	38.4	0.4289
Slope	3.98E-05			
K (m/s)	**6.11E-03**			

Q **2000 L/h**

PG **70** **kPa**
Area **0.2279** **m2**

time (sec)	DO (mg/L)	Temp (oC)	C* (mg/L)	LnY
0	2.01	24.2	44.27	0
1800	5.60	25.6	43.00	0.0917
3600	8.53	26.9	41.83	0.1788
5400	10.53	28.0	40.84	0.2477
7200	12.26	29.0	39.93	0.3151
9000	14.10	29.9	39.12	0.3942
10800	15.40	30.5	38.58	0.4559
Slope	4.19E-05			
K (m/s)	**6.43E-03**			

Q **2000 L/h**

PG **80** **kPa**
Area **0.2279** **m2**

time (sec)	DO (mg/L)	Temp (oC)	C* (mg/L)	LnY
0	2.33	20.3	47.80	0
1800	5.42	22.0	46.26	0.0729
3600	8.52	23.7	44.72	0.1579
5400	10.98	25.1	43.46	0.2361
7200	13.56	26.3	42.37	0.3292
9000	15.81	27.4	41.38	0.4234
10800	17.60	28.4	40.48	0.5113
Slope	4.77E-05			
K (m/s)	**7.33E-03**			

Q **2000 L/h**

PG **90** **kPa**
Area **0.2279** **m2**

time (sec)	DO (mg/L)	Temp (oC)	C* (mg/L)	LnY
0	2.35	21.1	47.07	0
1800	5.88	22.7	45.62	0.0851
3600	9.14	24.3	44.18	0.1771
5400	11.66	25.7	42.92	0.2607
7200	14.12	26.9	41.83	0.3540
9000	16.23	28.0	40.83	0.4474
10800	17.87	28.9	40.02	0.5310
Slope	4.95E-05			
K (m/s)	**7.60E-03**			

Q **2000 L/h**

PG **40** **kPa**
Area **0.2279** **m2**

time (sec)	DO (mg/L)	Temp (oC)	C* (mg/L)	LnY
0	2.08	23.4	45	0
1800	3.55	25	43.55	0.0361
3600	5.22	27	41.74	0.0825
5400	6.11	27.7	41.11	0.1090
7200	7.3	28.9	40.02	0.1480
9000	8.3	29.9	39.12	0.1838
10800	9.37	30.8	38.3	0.2247
Slope	2.05E-05			
K (m/s)	**3.15E-03**			

Q **2000 L/h**

PG **60** **kPa**
Area **0.2279** **m2**

time (sec)	DO (mg/L)	Temp (oC)	C* (mg/L)	LnY
0	2.04	24.4	44.09	0
1800	4.35	25.8	42.83	0.0583
3600	7.07	27.3	41.47	0.1365
5400	9.08	28	40.84	0.2002
7200	11.23	28.7	40.08	0.2765
9000	13.65	29.5	39.48	0.3712
10800	15.01	30	39.03	0.4318
Slope	4.09E-05			
K (m/s)	**6.28E-03**			

Q **2000 L/h**

PG **80** **kPa**
Area **0.2279** **m2**

time (sec)	DO (mg/L)	Temp (oC)	C* (mg/L)	LnY
0	2.17	22.8	45.53	0
1800	6.15	24.7	43.82	0.1004
3600	8.6	26	42.65	0.1730
5400	10.98	27	41.74	0.2519
7200	12.56	27.5	41.29	0.3087
9000	14.56	28	40.83	0.3864
10800	16.06	28.9	40.02	0.4572
Slope	4.13E-05			
K (m/s)	**6.34E-03**			

Q **2000 L/h**

Q **2000 L/h**

PG **50** **kPa**
Area **0.2279** **m2**

time (sec)	DO (mg/L)	Temp (oC)	C* (mg/L)	LnY
0	2.01	22.2	46.08	0
1800	4.01	24.2	44.27	0.0485
3600	6.59	25.7	42.92	0.1187
5400	8.98	27.4	41.38	0.1948
7200	11.05	28.3	40.57	0.2671
9000	12	29.5	39.48	0.3101
10800	13.01	30	39.03	0.3526

Slope	3.43E-05
K (m/s)	**5.27E-03**

Q **1500 L/h**

PG **30** **kPa**
Area **0.2279** **m2**

time (sec)	DO (mg/L)	Temp (oC)	C* (mg/L)	LnY
0	2.18	23.7	44.72	0
1800	3.01	24.5	44.00	0.02005
3600	3.52	26.7	42.01	0.03422
5400	4.04	28	40.84	0.04931
7200	4.47	29	39.93	0.06257
9000	4.98	30.2	38.85	0.07943
10800	5.36	30.9	38.22	0.09238
Slope	8.40E-06			
K (m/s)	**1.29E-03**			

Q **1500 L/h**

PG **40** **kPa**
Area **0.2279** **m2**

time (sec)	DO (mg/L)	Temp (oC)	C* (mg/L)	LnY
0	2.23	20.9	47.26	0
1800	2.92	23.5	44.91	0.0163
3600	3.44	26.2	42.46	0.0305
5400	3.9	28	40.83	0.0442
7200	4.47	29.6	39.39	0.0622
9000	4.93	31	38.12	0.0782
10800	5.62	32.3	39.86	0.0944
Slope	8.70E-06			
K (m/s)	**1.34E-03**			

Q **1500 L/h**

PG **50** **kPa**
Area **0.2279** **m2**

time (sec)	DO (mg/L)	Temp (oC)	C* (mg/L)	LnY
0	2.25	20.1	48	0
1800	3.45	22.5	45.81	0.0279
3600	4.68	25.9	42.74	0.0619
5400	6.01	27.8	41.02	0.1020
7200	7.86	28.1	40.75	0.1575
9000	8.06	31.8	37.4	0.1807
10800	9.67	32.3	37	0.2402

Slope	2.23E-05
K (m/s)	**3.42E-03**

Q **1500 L/h**

PG **60** **kPa**
Area **0.2279** **m2**

time (sec)	DO (mg/L)	Temp (oC)	C* (mg/L)	LnY
0	2.04	24.5	44	0
1800	3.7	26.8	41.92	0.0425
3600	5.12	28.5	40.39	0.0837
5400	6.67	30.5	38.58	0.1355
7200	7.86	31.5	37.67	0.1783
9000	8.93	32.8	36.5	0.2231
10800	10.01	33.6	35.78	0.2695

Slope	2.51E-05
K (m/s)	**3.85E-03**

Q **1500 L/h**

PG **70** **kPa**
Area **0.2279** **m2**

time (sec)	DO (mg/L)	Temp (oC)	C* (mg/L)	LnY
0	2.2	21	47.17	0
1800	3.98	23.2	45.18	0.0423
3600	5.65	25.4	43.19	0.0879
5400	8.78	27.8	41.02	0.1857
7200	10.02	30	39.03	0.2387
9000	12.96	31.7	37.49	0.3637
10800	13.58	33	36.32	0.4058

Slope	3.99E-05
K (m/s)	**6.13E-03**

Q **1500 L/h**

PG **80** **kPa**
Area **0.2279** **m2**

time (sec)	DO (mg/L)	Temp (oC)	C* (mg/L)	LnY
0	2.14	23.1	45.27	0
1800	4.31	25.4	43.19	0.0543
3600	6.64	27.4	41.38	0.1218
5400	9.09	29.4	39.57	0.2054
7200	10.72	31	38.13	0.2723
9000	13.29	33	36.39	0.3939
10800	15.05	33.8	35.6	0.4875

Slope	4.55E-05
K (m/s)	**6.99E-03**

Q **1500 L/h**

PG **90** **kPa**
Area **0.2279** **m2**

time (sec)	DO (mg/L)	Temp (oC)	C* (mg/L)	LnY
0	2.23	22.3	45.99	0
1800	5.18	24.7	43.82	0.0736
3600	8.64	27	41.74	0.1770
5400	10.55	28.7	40.21	0.2473
7200	12.59	30.4	38.67	0.3345
9000	14.33	31.7	37.49	0.4203
10800	16.01	32.9	36.4	0.5163

Slope	4.76E-05
K (m/s)	**7.31E-03**

Q **1000 L/h**

PG **40** **kPa**
Area **0.2279** **m2**

time (sec)	DO (mg/L)	Temp (oC)	C* (mg/L)	LnY
0	2.1	21	47.17	0
1800	2.98	23.1	45.27	0.0206
3600	3.35	25.7	42.92	0.0311
5400	4.01	26.9	41.83	0.0493
7200	4.28	28	40.84	0.0579
9000	4.65	29.2	39.75	0.0701
10800	5.24	31	38.13	0.0912

Slope	7.93E-06
K (m/s)	**1.22E-03**

Q **1000 L/h**

PG **50** **kPa**
Area **0.2279** **m2**

time (sec)	DO (mg/L)	Temp (oC)	C* (mg/L)	LnY
0	2.79	20.3	47.80	0
1800	3.91	23.3	45.09	0.0268
3600	4.65	26.1	42.56	0.0479
5400	5.5	28.8	40.11	0.0754
7200	6.17	30.7	38.40	0.0997
9000	6.74	32.5	36.77	0.1236
10800	7.3	33.7	35.69	0.1475

Slope	1.36E-05
K (m/s)	**2.09E-03**

Q **1000 L/h**

PG **60** **kPa**
Area **0.2279** **m2**

time (sec)	DO (mg/L)	Temp (oC)	C* (mg/L)	LnY
0	2.28	22.8	45.54	0
1800	3.25	25.3	43.28	0.0239
3600	5.01	28.5	40.39	0.0743
5400	5.99	30.3	38.76	0.1073
7200	7.48	33.6	35.78	0.1687
9000	8.58	34.2	35.23	0.2122
10800	8.93	35	34.51	0.2311
Slope	2.31E-05			
K (m/s)	**3.55E-03**			

Q **1000 L/h**

PG **70** **kPa**
Area **0.2279** **m2**

time (sec)	DO (mg/L)	Temp (oC)	C* (mg/L)	LnY
0	2.32	23.4	45.00	0
1800	2.62	26.1	42.56	0.0635
3600	4.12	28.1	40.75	0.1066
5400	6.54	30.8	38.31	0.1872
7200	8.52	33.1	36.23	0.2681
9000	9.43	34.3	35.14	0.3124
10800	11.03	35.2	34.33	0.3876
Slope	3.15E-05			
K (m/s)	**4.84E-03**			

Q **1000 L/h**

PG **80** **kPa**
Area **0.2279** **m2**

time (sec)	DO (mg/L)	Temp (oC)	C* (mg/L)	LnY
0	2.15	22.2	46.08	0
1800	3.73	25.2	43.37	0.0391
3600	5.66	27.7	41.11	0.0944
5400	7.55	29.9	39.12	0.1579
7200	9.55	31.9	37.31	0.2363
9000	11.47	33.4	36	0.3220
10800	13.68	34.9	34.6	0.4390
Slope	4.02E-05			
K (m/s)	**6.17E-03**			

Q **1000 L/h**

PG **90** **kPa**
Area **0.2279** **m2**

time (sec)	DO (mg/L)	Temp (oC)	C* (mg/L)	LnY
0	2.13	21.8	46.6	0
1800	5.5	24.8	43.73	0.0845
3600	7.92	27.3	41.47	0.1592
5400	10.53	30.2	38.84	0.2598
7200	12.33	31.9	37.31	0.3424
9000	14.51	33.3	36.05	0.4541
10800	16.63	35.4	34.15	0.6030
Slope	5.42E-05			
K (m/s)	**8.32E-03**			

Axial

PG **70** **kPa**
Area **0.2279** **m2**

time (sec)	DO (mg/L)	Temp (oC)	C* (mg/L)	LnY
0	2.3	22.8	45.54	0
1800	3.51	24.4	44.09	0.0294
3600	5.11	25.8	42.83	0.0719
5400	7.41	27.2	41.56	0.1394
7200	9.55	28.3	40.57	0.2101
9000	11.38	29.2	39.75	0.2776
10800	13.05	29.9	39.12	0.3453

Axial
Q **2000** **L/h**

PG **80** **kPa**
Area **0.2279** **m2**

time (sec)	DO (mg/L)	Temp (oC)	C* (mg/L)	LnY
0	2.08	25.5	43.10	0
1800	4.71	26.7	42.01	0.0681
3600	7.21	27.8	41.02	0.1413
5400	9.68	28.8	40.11	0.2229
7200	11.75	29.6	39.39	0.3000
9000	13.8	30.3	38.76	0.3850
10800	15.17	30.9	38.22	0.4498

APPENDIX C

Effect of aeration using air and oxygen

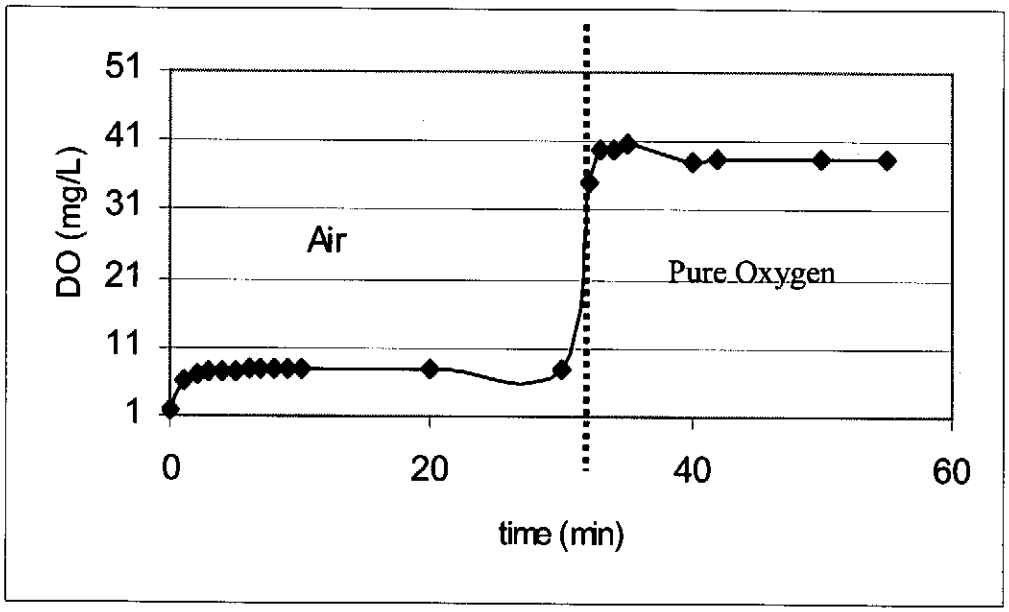

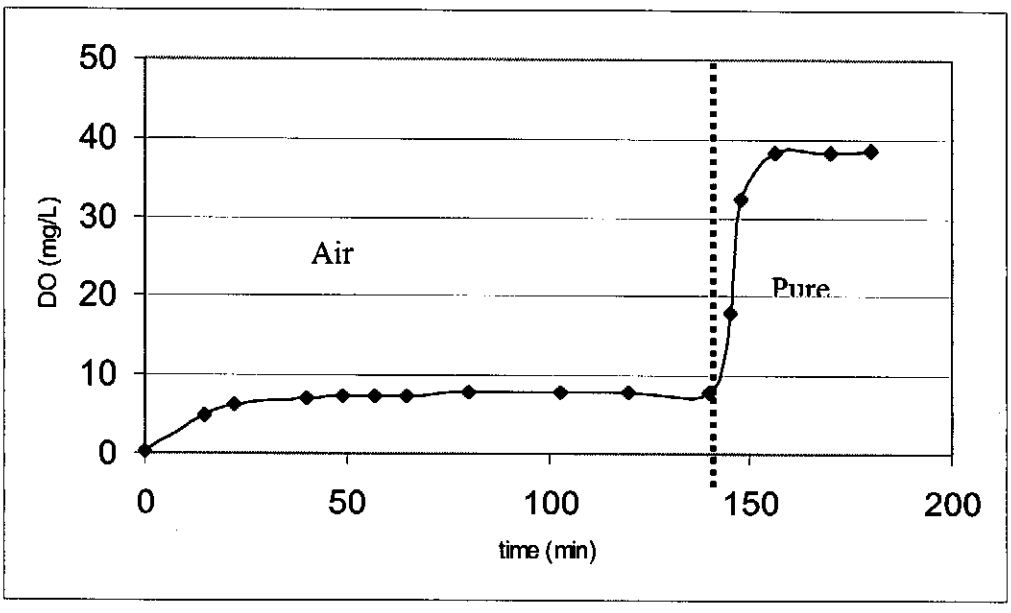

APPENDIX D

Experimental determination of permeability

Number of membranes 6

P1 = pressure applied to membrane lumen

P2 = atmospheric pressure

Area = 0.00105975m^2

P_1 (abs) kPa	P_1-P_2 kPa	Volume mL	Time min	Q m^3/s
111	11	5	45	1.85E-09
141	41	5	20	4.17E-09
141	41	5	16	5.21E-09
161	61	3	8	6.25E-09
171	71	3	7	7.14E-09
191	91	3	4	1.25E-08
191	91	3	4	1.25E-08
201	101	3	3	1.67E-08
Slope (KpA/X)	**2.00E-10**			
Kp/X $m^3/m^2.s.Pa$	**2.12E-13**			